Pure Appl. Chem., Vol. 71, No. 9, pp. 1771–1807, 1999.
Printed in Great Britain.

INTERNATIONAL UNION OF PURE AND APPLIED CHEMISTRY

ANALYTICAL CHEMISTRY DIVISION
COMMISSION ON ELECTROANALYTICAL CHEMISTRY

A CRITICAL EVALUATION OF THE REDOX PROPERTIES OF URANIUM, NEPTUNIUM AND PLUTONIUM IONS IN ACIDIC AQUEOUS SOLUTIONS

(Technical Report)

Prepared for publication by
SORIN KIHARA,[1] ZENKO YOSHIDA,[2] HISAO AOYAGI,[2] KOHJI MAEDA,[1] OSAMU SHIRAI,[3] YOSHIHIRO KITATSUJI[2] AND YUMI YOSHIDA[1]

[1]Department of Chemistry, Kyoto Institute of Technology, Matsugasaki, Sakyo, Kyoto 606–8585, Japan
[2]Tokai Establishment, Japan Atomic Energy Research Institute, Tokai, Ibaraki 319–1195, Japan
[3]Oarai Establishment, Japan Atomic Energy Research Institute, Oarai, Ibaraki 311–1394, Japan

A critical evaluation of the redox properties of uranium, neptunium and plutonium ions in acidic aqueous solutions (Technical Report)

Abstract: Standard redox potentials, E°s and redox processes of U, Np and Pu ions in acidic aqueous solutions are reviewed and evaluated critically. The E°s of reversible redox processes, MO_2^{2+}/MO_2^{+} and M^{4+}/M^{3+} (M: U, Np or Pu) adopted are those proposed mainly by Riglet *et al*. on the basis of the precise correction of formal potentials, $E^{\circ\prime}$s, according to the improved theoretical approach to estimate the activity coefficient. Electrode processes of the U, Np and Pu ions are discussed in terms of current–potential curves, measured so far by polarography, voltammetry or flow coulometry. Special attention is paid to the irreversible MO_2^{+}/M^{4+} reactions. Disproportionation reactions of MO_2^{+} are also discussed. New substances are introduced as intermediates during reductions of MO_2^{+} to M^{4+} or disproportionations of MO_2^{+}.

CONTENTS

1 INTRODUCTION

Uranium, neptunium and plutonium are dominant elements in the safe development of nuclear technology, since U and Pu are used as nuclear fuels, considerable amounts of Np and Pu are produced in the nuclear pile, Np and Pu have serious chemical toxicity, and nuclides, such as ^{237}Np or ^{239}Pu, are strong α-emitters of very long half lives.

The elements at the beginning of the actinides, i.e. U, Np and Pu, are characterized by the progressive filling of the 5*f* electron subshells which are more shielded than the 4*f* subshells of the lanthanides. The 5*f* and 6*d* electrons in these actinides are at similar energy levels because of the stabilization of 5*f* electrons, compared to that of 6*d* electrons, with increasing atomic number. Hence, 6*d* electrons are still involved in chemical bonding. Because of these features of U, Np and Pu, there are various oxidation states of the elements. Five oxidation states (3+ to 6+ and sometimes 7+) have been identified for these elements in aqueous solutions. Moreover, these oxidation states are liable to change with respect to disproportionation and oxidation by the dissolved oxygen or by reduction by the solvents. The ions in the aqueous solution behave as strong Lewis acids and those of oxidation states higher than 5+ form di- or tri-oxo ions.

In the present paper, standard potentials of U, Np and Pu ions in acidic aqueous solutions published so far are critically evaluated mainly from the view-point of the precise correction of formal potentials for activity coefficients by referring to the work of Riglet *et al*. [1,2]. Electrode processes of U, Np and Pu ions in acidic aqueous solutions are discussed by consulting both the current-potential curves reported on the basis of polarographic or voltammetric investigations and those obtained recently by the authors using flow coulometry. Deep understanding of redox behavior of the U, Np or Pu ions is considered to be one of the most important chemical subjects in the fields of a nuclear fuel preparation, the reprocessing of a spent nuclear fuel, and treatment of a nuclear waste, etc.

2 STANDARD REDOX POTENTIALS FOR URANIUM, NEPTUNIUM AND PLUTONIUM IONS IN ACIDIC AQUEOUS SOLUTIONS

Tables 1, 2 and 3 summarize literature values of the standard electrode potentials, E°s, of different U, Np and Pu redox couples in acidic aqueous solutions.

A classic reference of the E°s for actinides in water solutions is Latimer's 'Oxidation Potentials' [3] in which most of the E°s were estimated from thermodynamic data. Since, in the work of Latimer, not only the critical evaluation of the proposed data was not given by taking into account, e.g. formal potentials, $E^{\circ\prime}$s, determined electrochemically, but also many thermodynamic data used were estimated from those determined for elements other than actinides, such as lanthanides, many parts of Latimer's data have been rendered obsolete through modern publications.

The E°s for U, Np and Pu redox couples were revised after Latimer's work by applying new theories for prediction or evaluation of thermodynamic data, new techniques to determine $E^{\circ\prime}$s, and new theory for the correction of activities which is inevitable for estimation of E°s from $E^{\circ\prime}$s obtained by direct electrochemical measurements. By using new theories, one can re-evaluate a Gibbs energy, ΔG°, of the redox reaction based on the relation between ΔG° and the spectrometrically determined electron transfer band and/or *f-d* absorption band [4,5]. The re-evaluation was also carried out based on the hydration energy change estimated from the ionic radius, the charge of the ion and the modified ionic model which combines the standard enthalpy of formation of monoatomic gas, ionization potentials, the crystal ionic radius of metal and correlation parameters for different types of compound types [6–8]. The E°s obtained after Latimer's work were reviewed in the literature published in 1985 or 1986 [9,10]. Though the E° values given in the literature were evaluated by taking into account both the thermodynamic data and $E^{\circ\prime}$s determined electrochemically, the $E^{\circ\prime}$s were related to E°s by correcting for activity coefficients with the aid of empirical values or inadequate equations, without detailed discussion. Therefore, further discussion is required on the relation between E° and $E^{\circ\prime}$. The temperature dependencies of E°s, dE°/dT, are also open for discussion.

In the following, focusing our attention on the MO_2^{2+}/MO_2^{+} (M: U, Np or Pu), M^{4+}/M^{3+} and MO_2^{+}/M^{4+} redox couples which are especially important in the chemistry of M in acidic aqueous solutions, E°s are evaluated by extrapolating $E^{\circ\prime}$s determined based on electrochemical methods to the state of zero ionic strength referring mainly to the works by Riglet *et al*. [1,2]. Here, the authors consider that the electrochemical methods are promising for the direct study of precise features of redox reactions.

A temperature dependence of E°s is also discussed.

Table 1 Standard redox potentials, E°s, of uranium ions in acidic aqueous solution (V vs. NHE at 25 °C)

UO_2^{2+}/UO_2^{+}	UO_2^{+}/U^{4+}	UO_2^{2+}/U^{4+}	U^{4+}/U^{3+}	U^{3+}/U^{0}	U^{4+}/U^{0}	U^{3+}/U^{2+}	U^{2+}/U^{0}	UO_2^{+}/U^{3+}	UO_2^{2+}/U^{3+}	Ref.
+0.05	+0.62	+0.334	−0.61	−1.80						3
+0.163										17
+0.080	+0.558	+0.319	−0.596	−1.80				−0.019	+0.014	21
			−0.6			−4.7				4
				−1.70		−4.7	−0.2			5
+0.16	+0.38	+0.27	−0.52	−1.66	−1.38					9
+0.17	+0.38	+0.27	−0.52	−1.66	−1.38	−4.7	−0.1			10
			−0.6	−1.65	−1.40	−2.9	−1.02			8
+0.089										1
+0.160	+0.390	+0.273	−0.577	−1.642						28
(0.2)	(−3.4)	(−1.582)	(1.61)	(0.16)						

( ), Temperature coefficient, mV/K.

Table 2 Standard redox potentials, E°s, of neptunium ions in acidic aqueous solution (V vs. NHE at 25 °C)

NpO_2^{2+}/NpO_2^{+}	NpO_2^{+}/Np^{4+}	NpO_2^{2+}/Np^{4+}	Np^{4+}/Np^{3+}	Np^{3+}/Np^{0}	Np^{4+}/Np^{0}	Np^{3+}/Np^{2+}	NpO_3^{+}/NpO_2^{2+}	NpO_2^{+}/Np^{3+}	NpO_2^{2+}/Np^{3+}	Np^{2+}/Np^{0}	Ref.
+1.15	+0.75		+0.147	−1.86							3
+1.236											17
+1.153	+0.684	+0.918	+0.190	−1.83			>+2.1*	+0.437	+0.676		21
			+0.2			−4.7					4
				−1.81				+0.4			57
+1.24	+0.66	+0.95	+0.15	−1.79	−1.30		+2.04				9
+1.24	+0.64	+0.94	+0.15	−1.79	−1.30	−4.7	+2.04			−0.3	10
			+0.2	−1.78	−1.29	−2.9				−1.25	8
+1.160											1
+1.236	+0.567		+0.157	−1.768			+2.04				28
(0.058)	(−3.30)		(1.53)	(0.18)							
+1.162†			+0.210†								2
+1.161			+0.218								

* E° of NpO_2^{3+}/NpO_2^{2+}.
† E° at 20 °C.
( ), Temperature coefficient, mV/K.

Table 3 Standard redox potentials, E^0s, of plutonium ions in acidic aqueous solution (V vs. NHE at 25 °C)

PuO_2^{2+}/PuO_2^{+}	PuO_2^{+}/Pu^{4+}	PuO_2^{2+}/Pu^{4+}	Pu^{4+}/Pu^{3+}	Pu^{3+}/Pu^{0}	Pu^{4+}/Pu^{0}	Pu^{3+}/Pu^{2+}	PuO_3^{+}/PuO_2^{2+}	Pu^{2+}/Pu^{0}	PuO_2^{+}/Pu^{3+}	PuO_2^{2+}/Pu^{3+}	Ref.
+0.93	+1.15	+1.04	+0.97	−2.07							3
+1.013											17
+0.933	+1.115	+1.024	+1.017	−2.03			+0.857*		+1.066	+1.022	21
			+0.8			−3.5					4
				−1.96					+1.1		57
		+1.02									74
		+1.067									61
+1.02	+1.04	+1.03	+1.01	−2.00	−1.25						9
+1.02	+1.04	+1.03	+1.01	−2.00	−1.25	−3.5		−1.2			10
			+1.0	−1.97	−1.23	−2.9		−1.51			8
						−2.6					83
+0.940											1
+0.966.0	+1.035	+1.000	+1.006	−1.978		−2.8†	+2.4†	−1.6†	+1.021	+1.002	28
(0.03)	(−3.26)	(−1.615)	(1.441)	(0.23)		(+1.5)		(−0.4)	(−0.91)	(−0.596)	
+0.954‡			+1.015‡								2
+0.956			+1.026								

* E^0 of PuO_5^{3-}/PuO_4^{2-}.

† Uncertain value because the reaction involves doubtful species.

‡ E^0 at 20 °C.

( ), Temperature coefficient, mV/K.

2.1 Evaluation of E° from $E^{\circ\prime}$ determined by electrochemical measurements

Precise electrochemical data for ions of a high charge, e.g. most of actinide cations, can be obtained only in the presence of an inert electrolyte of fairly high concentration, usually 0.5–4 M (1 M = 1 mol/dm^3), and cannot be determined accurately or at all in dilute solutions. Therefore, it is important to solve the problem of converting data obtained for solutions of different ionic strengths and ionic compositions to a common reference solution state.

Riglet *et al*. [1,2] studied the MO_2^{2+}/MO_2^{+} and M^{4+}/M^{3+} couples polarographically or voltammetrically in acidic perchlorate solutions of various ionic strengths, and estimated E°s of these couples at $\mu = 0$ by correcting the $E^{\circ\prime}$s obtained for activity coefficients based on the Brønsted-Guggenheim-Scatchard specific ionic interaction theory (SIT) [11]. Here, μ denotes the dimensionless ionic strength, defined by the equation $\mu = (1/2)\Sigma_i(m_i/m^\circ)z_i^2$ where $m^\circ = 1$ mol/kg is the standard molality.

According to the SIT, the expression of the activity, γ, of an ion, i, of charge, z_i, is given as,

$$\log\gamma_i = -z_i^2 D + \sum_j \epsilon(\mathrm{i,j}) m_j \tag{1}$$

where, $D = 0.5107\mu^{1/2}/(1 + 1.5\mu^{1/2})$ is the Debye-Hückel term, ϵ(i,j) are the specific interaction coefficients between i and all the ions, j, of opposite charge, and m_j are molalities of j. When the concentration of the ions of the supporting electrolyte is much larger than the concentration of the reacting species, the supporting electrolyte makes the main contribution to the value of log γ_i. For a cation i in a ClO_4^- solution,

$$\log\gamma_i = -z_i^2 D + \epsilon(\mathrm{i}, ClO_4^-) m_{ClO_4^-} \tag{2}$$

The formal potential ($E^{\circ\prime}$) of the redox system, such as Eqn 3, can be connected to the standard potential (E°) by using γ_i in Eqn 2.

$$\mathrm{Ox} + \mathrm{ne} \rightleftharpoons \mathrm{Red} \tag{3}$$

$$E^{\circ\prime} = E^\circ + A[-\Delta z^2 D + \Delta\epsilon\ m_{ClO_4^-}] \tag{4}$$

where $A = RT/nF(\log e)$, $\Delta\epsilon = \epsilon(\mathrm{Ox},ClO_4^-) - \epsilon(\mathrm{Red},ClO_4^-)$ and $\Delta z^2 = {z_{Ox}}^2 - {z_{Red}}^2$.

Equation 4 indicates that the plot of $[(E^{\circ\prime}/A) + \Delta z^2 D]$ vs. $m_{ClO_4^-}$ is a straight line with intercept E°/A at $m_{ClO_4^-} = 0$ and slope $\Delta\epsilon$.

The $E^{\circ\prime}$s determined by Riglet *et al*. [1,2] are summarized in Tables 4 and 5 together with those reported by the other authors. Though $E^{\circ\prime}$s of the NpO_2^{2+}/NpO_2^{+}, PuO_2^{2+}/PuO_2^{+} and Pu^{4+}/Pu^{3+} couples given by Riglet *et al*. were those at 20 °C, these $E^{\circ\prime}$s can be converted to those at 25 °C by using the temperature dependencies of $E^{\circ\prime}$s determined by Connick & Mcvey [12], Cohen & Hindman [13,14], Riglet *et al*. [2] or Rabideau [15] (see Table 9). The converted values are also presented in Tables 4 and 5.

The plots of $[(E^{\circ\prime}/A) + \Delta z^2 D]$ vs. $m_{ClO4_4^-}$ gave straight lines when $E^{\circ\prime}$s given in Table 4 or 5 with § were employed, which indicates that many of the existing experimental determinations of $E^{\circ\prime}$s of MO_2^{2+}/MO_2^{+} or M^{4+}/M^{3+} couples could be well described by the SIT with constant interaction coefficients.

The E°s of MO_2^{2+}/MO_2^{+} and M^{4+}/M^{3+} couples estimated at $\mu = 0$ are listed in Tables 4 and 5, and ϵs reported or estimated and $\Delta\epsilon$ reported or surveyed according to Eqn 4 are summarized in Tables 6 and 7, respectively.

2.1.1 E° *of* MO_2^{2+}/MO_2^{+} *couples*

Fuger & Oetting [16] as well as Martinot & Fuger [9] proposed $+0.163 \pm 0.05$ V vs. NHE for E° of UO_2^{2+}/UO_2^{+} couple following the suggestion of Brand & Cobble [17] that all reported $E^{\circ\prime}$s for MO_2^{2+}/MO_2^{+} (M: U, Np, Pu, Am) couples in 1 M ClO_4^- solution should be corrected by 0.1 V in the estimation of E°s. Here, 0.1 V is the difference between E° of the NpO_2^{2+}/NpO_2^{+} couple, estimated by extrapolating $E^{\circ\prime}$ determined by the emf measurement to the infinite dilution [17], and the $E^{\circ\prime}$ measured by Sullivan *et al*. [18]. However, the value of 0.1 V is doubtful, since Brand & Cobble calculated E° by using activities of the pure electrolytes [$NpO_2(ClO_4)_2$, NpO_2ClO_4 and $HClO_4$] in the solution system and not their values

Table 4 Formal potentials, $E^{\circ\prime}$s, for the MO_2^{2+}/MO_2^{+} redox couples in perchlorate or chloride solutions determined electroanalytical techniques and standard electrode potentials, E^0s, at the ionic strength, $\mu = 0$

Redox system	Technique	Experimental details		Formal potential, $E^{\circ\prime}$ (V vs. NHE)	Standard potential, E° (V vs. NHE)	Ref.
		Solution	T (°C)			
UO_2^{2+}/UO_2^{+}	Pol	0.1 M Cl^- pH = 3	25	+0.062 ± 0.002	+0.081*	22
	Pol	0.1 M Cl^- pH = 2	25	+0.061 ± 0.001	+0.081*	23
	Pol	0.1 M ClO_4^- 0.05 M $HClO_4$	25	+0.067 ± 0.004§	+0.085*	27
	Pol	1 M ClO_4^- 0.05 M $HClO_4$	25	+0.063 ± 0.004§	+0.088*	27
	Pol	3 M ClO_4^- 0.05 M $HClO_4$	25	+0.074 ± 0.004	+0.081*	27
	Pol	0.5 M ClO_4^- 0.096 – 0.36 M $HClO_4$	25	+0.062 ± 0.002§	+0.088*	41
	Pol	3 M ClO_4^- 0.01 M $HClO_4$	25	+0.0811§		1
	Pol	2 M ClO_4^- 0.01 M $HClO_4$	25	+0.0709§		1
	Pol	1 M ClO_4^- 0.01 M $HClO_4$	25	+0.0654§	+0.089 ± 0.002	1
	Pol	0.5 M ClO_4^- 0.01 M $HClO_4$	25	+0.0623§		1
NpO_2^{2+}/NpO_2^{+}	Pot Pt	1 M HCl	25	+1.14 ± 0.02		54
	Emf Pt	1 M $HClO_4$	25	+1.1373 ± 0.0010§		13
	Emf Pt	1 M $HClO_4$	25	+1.13638 ± 0.00016§		18
	Emf Pt	0.091 M $HClO_4$	25	+1.239	+1.236 ± 0.01 (1.161 ± 0.008†)	17 2,17
	RV Pt	1 M $HClO_4$	20	+1.140 ± 0.007§		2
	CV Pt	1 M $HClO_4$	20	+1.140 ± 0.005§	+1.162 ± 0.011	2
	RV Pt	1 M $HClO_4$ +1 M $NaClO_4$	20	+1.149 ± 0.007§	(+1.161 ± 0.011‡)	2
	RV Pt	1 M $HClO_4$ +2 M $NaClO_4$	20	+1.162 ± 0.007§		2
PuO_2^{2+}/PuO_2^{+}	Emf Pt	1 M $HClO_4$	25	+0.925 ± 0.004		76
	Emf Pt	1 M ClO_4^- (pH = 3.4)	25	+0.935 ± 0.015		73
	Pot Pt	1 M $HClO_4$	25	+0.9164 ± 0.0002		15
	CV Pt	0.5 M $HClO_4$	20	+0.933 ± 0.005§		2
	CV Pt	1 M $HClO_4$	20	+0.941 ± 0.005§	+0.954 ± 0.010	2
	CV Pt	1 M $HClO_4$ +1 M $NaClO_4$	20	+0.951 ± 0.005§	(+0.956 ± 0.010‡)	2
	CV Pt	1 M $HClO_4$ +2 M $NaClO_4$	20	+0.967 ± 0.005§		2

* Corrected to $\mu = 0$ by using ϵ from Table 7.

† Recalculated based on SIT by Riglet *et al.* [2].

‡ Recalculated to the value characteristic for 25 °C using the temperature coefficient from Table 9.

Pol, polarography at the dropping mercury electrode; Pot Pt, potentiometry at a platinum electrode; Emf Pt, electromotive force measurement at a platinum electrode; RV Pt, voltammetry at a rotating platinum electrode; CV Pt, cyclic voltammetry at a platinum electrode.

§ The plots of $[(E^{\circ\prime}/A) + \Delta z^2 D]$ vs. $m_{ClO_4^-}$ gave straight lines when $E^{\circ\prime}$s given with § were employed (cf. Eqn 4).

Table 5 Formal potentials, $E^{\circ\prime}$s, for the M^{4+}/M^{3+} redox couples in perchlorate or chloride solutions determined by electroanalytical techniques and standard redox potentials, E°s, at the ionic strength, $\mu = 0$

Redox system	Technique	Experimental details		Formal potential, $E^{\circ\prime}$ (V vs. NHE)	Standard potential, E° (V vs. NHE)	Ref.
		Solution	T (°C)			
U^{4+}/U^{3+}	Pol	1 M HCl	25	-0.640 ± 0.005		27
	Pol	1 M $HClO_4$	25	-0.631 ± 0.005	-0.573*	2,27
					-0.607 ± 0.007	9,27
					-0.596	21,27
					$(-0.52 \pm 0.05$†)	9,27
Np^{4+}/Np^{3+}	Pot Hg	1 M HCl	25	$+0.137 \pm 0.005$		54
	Pol	1 M HCl	25	$+0.142 \pm 0.005$		53
	Emf Pt	1 M $HClO_4$	25	$+0.1551 \pm 0.0010$§	$+0.179 \pm 0.005$	9,13
					$+0.190 \pm 0.005$	13,21
	CV Pt	1 M $HClO_4$	25	$+0.154 \pm 0.005$§		2
	CV Pt	1 M $HClO_4$ +1 M $NaClO_4$	25	$+0.169 \pm 0.005$§	$+0.218 \pm 0.005$	2
	CV Pt	1 M $HClO_4$ +2 M $NaClO_4$	25	$+0.185 \pm 0.005$§		2
	CV Pt	0.5 M $HClO_4$	25	$+0.154 \pm 0.005$§		2
Pu^{4+}/Pu^{3+}	Pot Pt	1 M HCl	25	$+0.9703 \pm 0.0005$		26
	Emf Pt	0.1 M $HClO_4$	25	$+0.981 \pm 0.003$§	$+1.006 \pm 0.003$	9,25
					$+1.017 \pm 0.002$	21,25
	Emf Pt	1 M $HClO_4$	25	$+0.977 \pm 0.002$§		12
	Pot Pt	1 M $HClO_4$	25	$+0.9821 \pm 0.0005$§		26
	Emf Pt	0.5 M $HClO_4$	20	$+0.954 \pm 0.005$§		2
	CV Pt	1 M $HClO_4$	20	$+0.959 \pm 0.005$§	$+1.010 \pm 0.010$	2
	CV Pt	1 M $HClO_4$ +1 M $NaClO_4$	20	$+0.988 \pm 0.005$§	$(+1.026 \pm 0.010$‡)	2
	CV Pt	1 M $HClO_4$ +2 M $NaClO_4$	20	$+1.017 \pm 0.005$§		2

* Calculated by using ϵ from Table 7 (i.e., corrected by -0.631 ± 0.005 V for 0.058 V).

† Evaluated based on the Gibbs energy of formation.

‡ Recalculated to the value characteristics for 25 °C by using the temperature coefficient from Table 9.

Pol, polarography at the dropping mercury electrode; Pot Hg or Pot Pt, potentiometry using a mercury or platinum electrode; Emf Pt, electromotive force measurement at a platinum electrode; CV Pt, cyclic voltammetry at a platinum electrode.

§ The plots of $[(E^{\circ\prime}/A) + \Delta z^2 D]$ vs. m_{ClO4^-} gave straight lines when $E^{\circ\prime}$s given with § were employed (cf. Eqn 4).

in the mixture. Another difficulty is that Brand & Cobble estimated the activities based on the extended Debye-Hückel equation which is not appropriate to use in a concentrated solution, such as 1 M $HClO_4$.

Riglet *et al*. extrapolated their data on polarographic half-wave potentials, $E_{1/2}$, to $\mu = 0$ based on the SIT [1], and proposed $+0.089 \pm 0.002$ V vs. a normal hydrogen electrode, NHE, as E° of UO_2^{2+}/UO_2^{+} couple and $+0.18 \pm 0.02$ kg/mol as $\Delta\epsilon$ [$= \epsilon(UO_2^{2+},ClO_4^-) - \epsilon(UO_2^{+},ClO_4^-)$] at 25 °C. They estimated $\epsilon(UO_2^{+},ClO_4^-)$ to be $+0.28 \pm 0.04$ kg/mol by using the $\Delta\epsilon$ and $\epsilon(UO_2^{2+},ClO_4^-)$ reported as $+0.46 \pm 0.02$ kg/mol [19, 20].

By employing $\epsilon(MO_2^{2+},ClO_4^-) = +0.46 \pm 0.02$ kg/mol and $\epsilon(MO_2^{+},ClO_4^-) = +0.28 \pm 0.04$ kg/mol, we recalculated $E^{\circ\prime}$ reported for the UO_2^{2+}/UO_2^{+} couple in the literature to E° at $\mu = 0$, and the resulting data are listed in Table 4. The obtained E° values agreed well with that reported by Riglet *et al*. [1,2]. Accordingly, the difference between E° thus calculated and $E^{\circ\prime}$ determined is $+0.024 \pm 0.004$ V for 1 M ClO_4^- solution.

Table 6 Differences, $\Delta\epsilon$, between $\epsilon(MO_2^{2+},ClO_4^-)$ and $\epsilon(MO_2^{+},ClO_4^-)$ or $\epsilon(M^{4+},ClO_4^-)$ and $\epsilon(M^{3+},ClO_4^-)$, and differences between E° and $E^{\circ\prime}$ for the MO_2^{2+}/MO_2^{+} or M^{4+}/M^{3+} redox couple in 1 M ClO_4^-, ΔE, calculated based on $\Delta\epsilon$

$\Delta\epsilon$ (kg/mol)	ΔE (mV)	Ref.
$\epsilon(UO_2^{2+},ClO_4^-) - \epsilon(UO_2^{+},ClO_4^-) = 0.18 \pm 0.02$ at 25 °C	$+24 \pm 4$	1
	$(+26 \pm 2)$	
$\epsilon(NpO_2^{2+},ClO_4^-) - \epsilon(NpO_2^{+},ClO_4^-) = 0.21 \pm 0.03$ at 20 °C	+23	1,2
	$(+24 \pm 2)$	
	$+25 \pm 8$	13,18
$\epsilon(PuO_2^{2+},ClO_4^-) - \epsilon(PuO_2^{+},ClO_4^-) = 0.29 \pm 0.03$ at 20 °C	+24	2
	$(+19 \pm 2)$	
Mean $\epsilon(MO_2^{2+},ClO_4^-) - \epsilon(MO_2^{+},ClO_4^-) = 0.23 \pm 0.08$	$+22 \pm 6$	2
$\epsilon(Np^{4+},ClO_4^-) - \epsilon(Np^{3+},ClO_4^-) = 0.33 \pm 0.03$ at 20 °C	+66	2
0.35 ± 0.03 at 25 °C	+63	2
at 25 °C	$(+64 \pm 2)$	
$\epsilon(Pu^{4+},ClO_4^-) - \epsilon(Pu^{3+},ClO_4^-) = 0.54 \pm 0.03$ at 20 °C	$+53 \pm 8$	2
	$(+52 \pm 3)$	
Mean $\epsilon(M^{4+},ClO_4^-) - \epsilon(M^{3+},ClO_4^-) = 0.44 \pm 0.20$	$+58 \pm 15$	2

( ), Recalculated in the present work.

Table 7 Interaction coefficients, ϵ(i,j)

i	j	ϵ (kg/mol)	Ref.
UO_2^{2+}	ClO_4^-	0.46 ± 0.02	19,20
UO_2^{2+}	Cl^-	0.21	20
UO_2^{+}	ClO_4^-	0.28 ± 0.04	1
UO_2^{+}	Cl^-	0.13*	1
(M=U, Np, Pu)			
MO_2^{2+}	ClO_4^-	0.46 ± 0.02	1,2,19,20
MO_2^{+}	ClO_4^-	0.28 ± 0.04	1
		0.23 ± 0.10	2
$M^{3+}(=Y^{3+})$	ClO_4^-	0.49 ± 0.04	2,24
M^{4+}	ClO_4^-	0.92 ± 0.24	2

* Based on the assumption of: $\epsilon\,(UO_2^{2+},ClO_4^-)/\epsilon\,(UO_2^{+},ClO_4^-) = \epsilon\,(UO_2^{2+},Cl^-)/\epsilon\,(UO_2^{+},Cl^-)$.

Riglet *et al*. recalculated Brand & Cobble's data by using the SIT and extrapolating these data to $\mu = 0$ [1,2], and proposed $+1.161 \pm 0.008$ V vs. NHE as E° of the NpO_2^{2+}/NpO_2^{+} couple at 25 °C. The difference between the E° (NpO_2^{2+}/NpO_2^{+}) thus proposed and $E^{\circ\prime}$ for 1 M ClO_4^- reported by Sullivan *et al*. [18] or Cohen & Hindman [13] is $+0.025 \pm 0.008$ V which is identical with the difference for the UO_2^{2+}/UO_2^{+} couple. Riglet *et al*. also extrapolated various experimental data including their own data (summarized in Table 4) to $\mu = 0$ based on SIT. They obtained $+1.162 \pm 0.011$ V and $+0.954 \pm 0.010$ V vs. NHE as E°s of NpO_2^{2+}/NpO_2^{+} and PuO_2^{2+}/PuO_2^{+} couples, respectively, at 20 °C and $\Delta\epsilon$ values as listed in Table 6. Here, the dependence of $\Delta\epsilon$ on temperature between 20 and 25 °C was assumed to be negligible compared with the experimental error.

Basing on the results described above, Riglet *et al*. [2] proposed that $E^{\circ\prime}$s of the MO_2^{2+}/MO_2^{+} couples of all M in 1 M ClO_4^- solution should be corrected by a constant equal to $+0.022 \pm 0.006$ V, and that the ϵ-values for all M of the same oxidation state and chemical form were identical in a given solution. That

is, $\epsilon(MO_2^{+},ClO_4^{-})$ for all of M were assumed to be $+0.23 \pm 0.10$ kg/mol by employing $+0.23 \pm 0.08$ kg/mol as $\Delta\epsilon$ which was the mean of $\Delta\epsilon$ calculated for U, Np and Pu (cf. Table 6) and $+0.46 \pm 0.02$ kg/mol as $\epsilon(MO_2^{2+},ClO_4^{-})$ for all of M which was the value reported for $\epsilon(UO_2^{2+},ClO_4^{-})$. The E° values for the MO_2^{2+}/MO_2^{+} couples found by Riglet *et al*. [2] by adopting the above-indicated $\epsilon(MO_2^{2+},ClO_4^{-})$ and $\epsilon(MO_2^{+},ClO_4^{-})$ are also consistent with those proposed for U, Np and Pu by Ahrland *et al*. [21], and that calculated for Am by Martinot & Fuger [9] from the enthalpy and entropy data. Agreement of E° values determined by different ways supports the correction of $+0.022 \pm 0.006$ V rather than 0.1 V is suitable for conversion of $E^{\circ\prime}$s for the MO_2^{2+}/MO_2^{+} couples in 1 M ClO_4^{-} to E° values at $\mu = 0$. Hence, the value $\epsilon(MO_2^{2+},ClO_4^{-}) - \epsilon(MO_2^{+},ClO_4^{-}) = +0.23 \pm 0.08$ kg/mol may be reasonable for all M.

The E° for the UO_2^{2+}/UO_2^{+} couple was estimated from $E^{\circ\prime}$ obtained in the Cl^- solutions [22,23] to be + 0.081 V vs. NHE by correcting for $\epsilon(UO_2^{2+},Cl^-) = +0.21$ kg/mol which was reported in literature [19] and $\epsilon(UO_2^{+},Cl^-) = +0.13$ kg/mol which was estimated by assuming $\epsilon(UO_2^{2+},ClO_4^{-})/\epsilon(UO_2^{+},ClO_4^{-}) = \epsilon(UO_2^{2+},Cl^-)/\epsilon(UO_2^{+},Cl^-)$.

2.1.2 E$^{\circ\prime}$*s of the* M^{4+}/M^{3+} *couples*

In most publications before that of Riglet *et al*. [2], the E°s of the M^{4+}/M^{3+} (M: U, Np or Pu) couples were determined only at one ionic strength.

Riglet *et al*. determined $E^{\circ\prime}$s for the M^{4+}/M^{3+} (M: Np, Pu) couples in the ClO_4^{-} solutions of various ionic strengths, 0.5 M < μ < 3.0 M ClO_4^{-}, at 25 or 20 °C as listed in Table 5. The plots of $[(E^{\circ\prime}/A) + \Delta z^2 D]$ vs. $m_{ClO_4^-}$ were linear [cf. Eqn 4] when $E^{\circ\prime}$s (or $E^{\circ\prime}$s converted to values at 25 °C), reported by Riglet *et al*. and other authors which are listed with § in Table 5, were employed. The E°s at 25 °C determined from the intercepts at $\mu = 0$ of the straight lines were $+0.218 \pm 0.005$ V for Np^{4+}/Np^{3+} couple and $+1.026 \pm 0.010$ V vs. NHE for Pu^{4+}/Pu^{3+} couple. The values of $\Delta\epsilon = \epsilon(M^{4+},ClO_4^{-}) - \epsilon(M^{3+},ClO_4^{-})$ were estimated from the slopes of the lines to be those in Table 6. Though the difference of $\Delta\epsilon$ between two M^{4+}/M^{3+} systems is rather large, Riglet *et al*. assumed the $\Delta\epsilon$s at 20–25 °C for all actinides to be the mean of these values (= 0.44 ± 0.20 kg/mol) considering that ϵ-value is the same for all actinides of the same oxidation state under the same solution conditions. Accepting the $\Delta\epsilon$ and assuming $\epsilon(M^{3+},ClO_4^{-})$ is identical with $\epsilon(Y^{3+},ClO_4^{-}) = 0.49 \pm 0.04$ kg/mol [24], $\epsilon(M^{4+},ClO_4^{-})$ is derived as 0.92 ± 0.24 kg/mol.

The $\Delta\epsilon$ (= 0.44 ± 0.20 kg/mol) suggests that E°s of the M^{4+}/M^{3+} couples should be obtained by making a constant correction of 0.058 ± 0.012 V for their $E^{\circ\prime}$s in a 1 M ClO_4^{-} solution. This correction seems to be preferred over +0.024 V proposed by Martinot & Fuger [9], since +0.024 V was determined based on E° obtained with Pu^{4+}/Pu^{3+} couple in 0.1 M $HClO_4$ solution [25] where the hydrolysis of Pu^{4+} is not negligible, or based on E° which had not been corrected for the hydrogen ion activity in the $HClO_4$ solution [26].

The only $E^{\circ\prime}$ of U^{4+}/U^{3+} couple in 1 M $HClO_4$ reported is -0.631 ± 0.005 V vs. NHE [27]. The correction of this $E^{\circ\prime}$ for 0.058 ± 0.012 V gives E° of -0.573 ± 0.017 V which is identical with that (−0.577 V vs. NHE) proposed by Bratsch [28].

2.1.3 E$^\circ$ *of the* MO_2^{2+}/M^{4+}, MO_2^{+}/M^{4+}, MO_2^{2+}/M^{3+} *or M(VII)/*MO_2^{2+} *couples*

The $E^{\circ\prime}$ values of these couples are difficult to determine by voltammetry or polarography since the electrode reactions of the MO_2^{2+}/M^{4+}, MO_2^{+}/M^{4+} or MO_2^{2+}/M^{3+} couples are highly irreversible, and $E^{\circ\prime}$s of the M(VII)/MO_2^{2+} couples are very positive. Hence, the $E^{\circ\prime}$ data available on these couples are limited. Table 8 summarizes $E^{\circ\prime}$s determined by electrochemical or thermodynamic methods and E°s evaluated from $E^{\circ\prime}$s.

The difference between E° and $E^{\circ\prime}$ of the MO_2^{+}/M^{4+} couple was calculated by using SIT based on assumption that $\epsilon(MO_2^{+},ClO_4^{-}) = +0.28 \pm 0.04$ and $\epsilon(M^{4+},ClO_4^{-}) = +0.92 \pm 0.24$ kg/mol. It was estimated that $E^{\circ\prime}$ for 1 M $HClO_4$ is by 0.143 ± 0.016 V more positive than E°. The estimated E°s are also presented in Table 8.

Summarizing the above discussion, we recommend E°s of the MO_2^{2+}/MO_2^{+}, M^{4+}/M^{3+} and MO_2^{+}/M^{4+} couples in acidic aqueous solutions calculated based on SIT and using the $\Delta\epsilon$ and ϵ-values listed in Tables 6 and 7, though further discussion is required, especially on the correction of activity coefficients to connect $E^{\circ\prime}$ with E°.

Table 8 Formal potentials, $E^{\circ\prime}$s, for the MO_2^{2+}/M^{4+}, MO_2^{+}/M^{4+}, MO_2^{2+}/M^{3+} or MO_3^{+}/MO_2^{2+} redox couples in perchlorate or chloride solutions and standard redox potentials, E°s, at $\mu = 0$

Redox system	Technique	Experimental details		Formal potential, $E^{\circ\prime}$ (V vs. NHE)	Standard redox potential, E° (V vs. NHE)	Ref.
		Solution	T (°C)			
UO_2^{2+}/U^{4+}	Emf Pt	1.0 M $HClO_4$	25	+0.3380	+0.3273 ± 0.001	77,78
					+0.195*	77
	ΔG		25		+0.273 ± 0.005	9
NpO_2^{+}/Np^{4+}	Emf Pt	1.0 M $HClO_4$	25	+0.7391 ± 0.0005	+0.684	14,21
					+0.670 ± 0.060	9,14
					+0.596*	14
	Pot Pt	1.0 M HCl	25	+0.737 ± 0.006		54
	ΔG		25		+0.65 ± 0.08	9
NpO_3^{+}/NpO_2^{2+}	Emf Pt	1.0 M $HClO_4$	25	+2.04 ± 0.003		79
PuO_2^{+}/Pu^{4+}	Pot Pt	1.0 M $HClO_4$	25	+1.1721	+1.03*	15
				(+1.010 ± 0.010†)	+0.867*	2,15
	ΔG	1.0 M $HClO_4$	25	+1.042 ± 0.001		9
	ΔG		25		+1.032 ± 0.037	9
PuO_2^{2+}/Pu^{3+}	ΔG	1.0 M $HClO_4$	25	+1.022 ± 0.0016		9

* Calculated in this work from $E^{\circ\prime}$ in Refs [2,14,15 or 77] by using ϵ from Table 7.
† Recalculated by Riglet *et al.* [2].
Emf Pt, electromotive force measurement at a platimun electrode; ΔG, evaluated based on the Gibbs energy of formation; Pot Pt, potentiometry at a platinum electrode.

2.2 Temperature dependence of E°

The temperature dependence of E°, $\Delta E^{\circ}/\Delta T$, can be estimated to be $\Delta E^{\circ}/\Delta T \approx \Delta S^{\circ}/nF$ for the n electron process based on the Gibbs-Helmholtz relation, $S^{\circ} = -(\partial G^{\circ}/\partial T)_{p,n_i}$. The $\Delta E^{\circ}/\Delta T$ values for redox couples of U, Np and Pu at $\mu = 0$ were estimated by Riglet *et al*. [2] by using ΔS°s from the literature or those calculated from ΔG°s and ΔH°s in the literature. Bratsch [28] also reviewed $\Delta E^{\circ}/\Delta T$ on the basis of critical evaluation of E°. These results are listed in Table 9 together with those on the $\Delta E^{\circ}/\Delta T$ reported from the direct experiments. Though there exists significant discrepancy among $\Delta E^{\circ}/\Delta T$ calculated from thermodynamic data and those determined experimentally, the results suggest that $\Delta E^{\circ}/\Delta T$ is constant for a given redox couple within the actinides investigated.

3 REDOX REACTIONS OF URANIUM, NEPTUNIUM AND PLUTONIUM IN ACIDIC AQUEOUS SOLUTIONS INVESTIGATED BY POLAROGRAPHY OR VOLTAMMETRY

Generally, the measurements of current-potential relations by voltammetry, polarography or related methods are very important not only to elucidate the reaction mechanism and estimate the reaction rate but also to determine E° from $E^{\circ\prime}$.

Current-potential curves of MO_2^{2+}/MO_2^{+} and M^{4+}/M^{3+} (M: U, Np or Pu) in acidic aqueous solutions in the absence of special complexing agents were investigated by polarography at the dropping mercury electrode, DME, voltammetry at the platinum or carbon electrode or related techniques. The electrode processes of these couples are fast, i.e. reversible or somewhat quasi reversible. The reduction of UO_2^{2+} to U^{4+} was also studied polarographically and the reaction was found to be irreversible. The $E^{\circ\prime}$ or half-wave potentials, $E_{1/2}$, reported so far are summarized in Tables 4, 5 and 10.

There are very few reports on current-potential curves of MO_2^{+}/M^{4+} measured by conventional polarographic or voltammetric techniques, since these redox processes are totally irreversible due to the breaking or forming of the metal–oxygen bonds. The current-potential curves for these irreversible couples reported so far were for uranium in hydrochloric acid [27] or sulfanilate-buffered solutions [29]

Table 9 Temperature coefficients of E°s, $\Delta E^\circ/\Delta T$, in mV/K, at 298 K

Redox reaction	$\Delta E^\circ/\Delta T$				
	From $\Delta S^\circ/F$*	From $(\Delta H^\circ - \Delta G^\circ)/FT$*	Recommended by Bratsh [28]	From direct measurement	Ref.
UO_2^{2+}/UO_2^{+}	0.08 ± 0.54	0.75 ± 0.12	(0.2)		
NpO_2^{2+}/NpO_2^{+}	0.07 ± 0.69	0.76 ± 0.17	0.058	−0.3	13
PuO_2^{2+}/PuO_2^{+}	0.03 ± 0.97	0.74 ± 0.17	0.03	+0.4	15
U^{4+}/U^{3+}	1.80 ± 0.48	2.48 ± 0.28	1.61		
Np^{4+}/Np^{3+}	1.50 ± 0.59	2.18 ± 0.28	1.53	+1.3	13
				+1.6	2
Pu^{4+}/Pu^{3+}	1.42 ± 0.38	2.12 ± 0.29	1.441	+2.2	12
UO_2^{2+}/U^{4+}			(−3.4)		
NpO_2^{2+}/Np^{4+}			−3.30		
PuO_2^{2+}/Pu^{4+}			−3.26		

( ), Estimated.
* $\Delta E^\circ/\Delta T$ calculated by Riglet *et al.* [2] based on ΔS°, ΔH° and ΔG° given in [9,10,16,87].

by polarography, for neptunium in sulphuric acid [30] by coulometry with the aid of a thin-layer cell with conducting glass electrodes, for relatively concentrated plutonium (0.016–0.025 M) in perchloric acid [31] by controlled potential electrolysis at a platinum electrode as well as for uranium, neptunium and plutonium by flow coulometry at the column electrode with the glassy carbon fiber working electrode by the present authors [32–35].

3.1 Uranium

The characteristics of polarographic waves of uranium in various solutions reported since the first work of Herasymenko [36] till 1950 were reviewed by Booman *et al*. [37].

Two polarographic waves were observed at DME for UO_2^{2+} in a moderately acidic aqueous solution (0.01–0.1 M hydrochloric acid) with $E_{1/2}$ at −0.18 and −0.92 V vs. the saturated calomel electrode, SCE. The 1st wave was independent of the acid concentration, c_{H^+}, the concentration of UO_2^{2+}, $c_{UO_2^{2+}}$, or presence of potassium chloride at concentration up to 0.5 M. Hence, the 1st wave was attributed to the reversible reduction, as Eqn 5 [38–40].

$$UO_2^{2+} + e \rightleftharpoons UO_2^{+} \tag{5}$$

The 2nd wave was about twice as large as the 1st wave. Its $E_{1/2}$-value was independent of c_{H^+}, but depended slightly on $c_{UO_2^{2+}}$, indicating somewhat irreversible characteristics. The wave was postulated as a composite due to reactions (6) and (7) or (8) [38–40].

$$UO_2^{+} + 4H^+ + e \rightarrow UO^{2+} + 2H_2O \tag{6}$$

$$UO^{2+} + e \rightarrow UO \tag{7}$$

or

$$UOOH^{+} + e \rightarrow UOOH \tag{8}$$

In a more acidic electrolyte, i.e. for c_{H^+} higher than 0.2 M, the height of the 1st wave increased with increasing acidity at the expense of that of the 2nd wave, owing to the disproportionation of UO_2^{+}.

Kern & Orlemann [41] found that mixtures of UO_2^{+} and UO_2^{2+} in acidic perchlorate solutions produced a reversible anodic and cathodic wave, and concluded that the E° value for the UO_2^{2+}/UO_2^{+} couple was +0.062 ± 0.002 V vs. NHE which agreed exactly with the value determined by Kritchevsky & Hindman [27]. They utilized the well-defined anodic diffusion current of UO_2^{+} to study the kinetics of

Table 10 Characteristics of typical polarograms or voltammograms for the uranium, neptunium and plutonium ions in acidic aqueous solutions

Redox couple	Solution	Electrode	Technique	Temp. (°C)	Half-wave potential, peak potential or quarter-wave potential (V) [Reference electrode]	Reversibility	Ref.	Remarks
Uranium								
$UO_2^{2+} \rightarrow UO_2^{+}$	0.1 M HCl	DME	DC Pol	25	$E_{1/2} = -0.183$ [SCE]	Reversible	80	
	0.1 M HCl	DME	DC Pol	25	$E_{1/2} = -0.176$ [SCE]	Reversible	27	$E_{1/2}$: Independent of pH
	0.1 M HCl + 0.1 M KCl	DME	DC Pol	25	$E_{1/2} = -0.180$ [SCE]	Reversible	38	$D(UO_2^{2+}) = 0.62 \times 10^{-5}$ cm^2/s
	0.1 M $HClO_4$ (pH = 2.3)	DME	DC Pol		$E_{1/2} = -0.17$ [SCE]	Reversible	29	
	0.1 − 0.5 M $HClO_4$ $\mu = 0.5$	DME	DC Pol	25	$E_{1/2} = -0.066$ [SCE]	Reversible	80	$E_{1/2}$: Independent of pH
	0.1 M $HClO_4$	DME	DC Pol	25	$E_{1/2} = -0.175$ [SCE]	Reversible	27	$E_{1/2}$: Independent of pH and $[ClO_4^-]$
	0.1 M HNO_3	DME	DC Pol		$E_{1/2} = -0.165$ [SCE]	Quasi reversible	46	$D(UO_2^{2+}) = 1.05 \times 10^{-5}$cm^2/s
	2.0 M HNO_3	DME	DC Pol		$E_{1/2} = -0.164$ [SCE]	Quasi reversible	46	
	0.05 M H_2SO_4	DME	DC Pol		$E_{1/2} = -0.22$ [SCE]		80,81	$E_{1/2}$: Dependent on acid concentration
	0.1 M H_3PO_4 + 0.1 M HCl	DME	DC Pol		$E_{1/2} = -0.2$ [SCE]		80	
	1 − 9 M H_3PO_4	DME	DC Pol	22	$E_{1/2} = -0.180$ [SCE] in 1.2×10^{-3} M UO_2^{2+} + 1 M H_3PO_4	Quasi reversible	52	$D(UO_2^{2+}) = 1.80 \times 10^{-5}$ cm^2/s $E_{1/2}$: Dependent on $[UO_2^{2+}]$ and $[H_3PO_4]$
$UO_2^{2+} \rightarrow$ U(IV)	2 M HCl	DME	DC Pol		$E_{1/2} = -0.213$ [SCE]		80	
	0.5 M H_2SO_4	DME	DC Pol		$E_{1/2} = -0.19$ [SCE]		81	
$UO_2^{+} \rightarrow$ U(IV)	0.05 M H_2SO_4	DME	DC Pol		$E_{1/2} = -0.9$ [SCE]		80,81	
$UO_2^{+} \rightarrow$ U(III)	0.1 M HCl	DME	DC Pol		$E_{1/2} = -0.94$ [SCE]		80	
	0.01 M HCl + 0.1 M KCl	DME	DC Pol		$E_{1/2} = -0.92$ [SCE]		38	
	0.1 M HCl	DME	DC Pol	25	$E_{1/2} = -0.820$ [SCE]	Composed of 2 waves	27	Effect of a maximum suppresser is remarkable
	0.1 M $HClO_4$	DME	DC Pol	25	$E_{1/2} = -0.839$ [SCE]	Composed of 2 waves	27	
U(IV) → U(III)	0.1 M HCl	DME	DC Pol	25	$E_{1/2} = -0.885$ [SCE]	Reversible	27	

Table 10 *Continued*

	1 M HCl	DME	DC Pol	25	$E_{1/2}$= −0.891 [SCE]	Reversible	27	
	2 M HCl	DME	DC Pol		$E_{1/2}$= −0.9 [SCE]		80	
	0.1 M $HClO_4$	DME	DC Pol	25	$E_{1/2}$= −0.862 [SCE]	Reversible	27	$D(U^{4+}) = 0.66 \times 10^{-5}$ cm^2/s $D(U^{3+}) = 0.65 \times 10^{-5}$ cm^2/s
	0.1 M $HClO_4$	DME	DC Pol	25	$E_{1/2}$= −0.93 [SCE]		80	
	1 M $HClO_4$	DME	DC Pol	25	$E_{1/2}$= −0.878 [SCE]	Reversible	27	
	0.05 M H_2SO_4	DME	DC Pol		$E_{1/2}$= −1.06 [SCE]		80	
	0.1 M H_2SO_4 + 0.1 M KCl	DME	DC Pol		$E_{1/2}$= −0.97 [SCE]	Reversible	82	
U(IV) ← U(III)	1 M HCl	DME	DC Pol	25	$E_{1/2}$= −0.877 [SCE]	Reversible	27	
	0.1 M HCl	DME	DC Pol		$E_{1/2}$= −0.93 [SCE]		80	
	1 M $HClO_4$	DME	DC Pol	25	$E_{1/2}$= −0.873 [SCE]	Reversible	27	
	0.1 M H_2SO_4 + 0.1 M KCl	DME	DC Pol		$E_{1/2}$= −0.97 [SCE]	Reversible	82	
UO_2^+ ← U(IV)	0.02 − 0.2 M $HClO_4$ + 0.1 M $NaClO_4$ Sulfanilate buffer	DME	DC Pol	25	$E_{1/2}$= E^0 − 0.118 pH		29	
U(III) → U^0		DME	Radio pol		$E_{1/2}$= −1.65 [NHE]		5	
Neptunium								
NpO_2^{2+}→NpO_2^+	0.5 M $HClO_4$	GC	CV		E_{pc} = +0.95 [SSE]	Reversible	60	
	1 M HNO_3	GC	CV		E_{pc} = +0.98 [SSE]	Reversible	60	
	0.5 M H_2SO_4	GC	CV		E_{pc} = +0.91 [SSE]	Not quite reversible	60	
	1 M H_2SO_4	Conducting glass electrode	CTLC Coulo		$E_{1/2}$= +0.42 [MSE] = +0.84 [SCE]	Reversible	30	
NpO_2^{2+} ← NpO_2^+	0.5 M $HClO_4$	GC	CV		E_{pa} = +1.01 [SSE]	Reversible	60	
	1 M HNO_3	GC	CV		E_{pa} = +1.04 [SSE]	Reversible	60	
	0.5 M H_2SO_4	GC	CV		E_{pa} = +1.02 [SSE]	Not quite reversible	60	
	1 M H_2SO_4	Conducting glass electrode	CTLC Coulo		$E_{1/2}$= +0.42 [MSE] = +0.84 [SCE]	Reversible	30	
Np(IV) → Np(III)	1 M HCl	DME	DC Pol	25	$E_{1/2}$= −0.104 ± 0.003 [SCE]	Reversible	53	
	0.1 M HCl + 0.9 M NaCl	DME	DC Pol	25	$E_{1/2}$= −0.101 ± 0.0003 [SCE]	Reversible	53	

Table 10 *Continued*

	1 M $HClO_4$	DME	DC Pol	25	$E_{1/2}$= −0.099 ± 0.006 [SCE]	Not quite reversible	53	$D(Np^{4+}) = 0.56 \times 10^{-5}$ cm^2/s
	5 M $HClO_4$	DME	DC Pol	25	$E_{1/2}$= −0.044 to −0.060 [SCE]	Not quite reversible	53	
	0.5 M $HClO_4$	GC	CV		E_{pc} = −0.02 [SSE]	Not quite reversible	60	
	1 M HNO_3	GC	CV		E_{pc} = −0.08 [SSE]	Reversible	60	
	0.5 M H_2SO_4	GC	CV		E_{pc} = −0.23 [SSE]	Quasi reversible	60	
	1 M H_2SO_4	Conducting glass electrode	CTLC Coulo		$E_{1/2}$= −0.7 [MSE] = −0.29 [SCE]	Reversible	30	
Np(IV) ←Np(III)	1 M HCl	DME	DC Pol	25	$E_{1/2}$= −0.102 ± 0.001 [SCE]	Reversible	53	
	0.1 M HCl + 0.9 M NaCl	DME	DC Pol	25	$E_{1/2}$= −0.101 [SCE]	Reversible	53	
	1 M $HClO_4$	DME	DC Pol	25	$E_{1/2}$= −0.064 ± 0.005 [SCE]	Not quite reversible	53	$D(Np^{3+}) = 0.645 \times 10^{-5}$ cm^2/s
	0.5 M $HClO_4$	GC	CV		E_{pa} = +0.05 [SSE]	Not quite reversible	60	
	1 M HNO_3	GC	CV		E_{pa} = −0.02 [SSE]	Reversible	60	
	0.5 M H_2SO_4	GC	CV		E_{pa} = −0.095 [SSE]	Quasi reversible	60	
	1 M H_2SO_4	Conducting glass electrode	CTLC Coulo		$E_{1/2}$= −0.7 [MSE] = −0.29 [SCE]	Reversible	30	
Plutonium								
$PuO_2^{2+} \rightarrow PuO_2^{+}$	1 M $HClO_4$	Pt	Chronopot	25.8	$E_{\tau/4}$= +0.39 to +0.56 [SCE]	Not quite reversible	64	$D(PuO_2^{2+}) = (0.72 \pm 0.3) \times 10^{-5}$ cm^2/s $E_{\tau/4}$: Dependent on current density
$PuO_2^{2+} \rightarrow$ Pu(III)	1 M $HClO_4$	Pt	Chronopot	25.8	$E_{\tau/4}$= −0.30 to −0.40 [SCE]	Not quite reversible	64	$E_{\tau/4}$: Dependent on current density
Pu(IV) → Pu(III)	1 M HCl	Pt	Chronopot	28.9	$E_{\tau/4}$= +0.74 [SCE]	Not quite reversible	64	$D(Pu^{4+}) = (0.52 \pm 0.02) \times 10^{-5}$ cm^2/s $E_{\tau/4}$: Slightly dependent on current density
	1 M HCl	Pt	Sq vol		$E_{1/2}$= +0.71 [SCE]	Not quite reversible	63	
	1 M $HClO_4$	Pt	Chronopot	26.3	$E_{\tau/4}$= +0.73 [SCE]	Not quite reversible	64	$D(Pu^{4+}) = (0.47 \pm 0.01) \times 10^{-5}$ cm^2/s $E_{\tau/4}$: Slightly dependent on current density

Table 10 *Continued*

	1 M HNO_3	Pt	Chronopot	25.8	$E_{\tau/4}$= +0.69 [SCE]	Not quite reversible	64	$D(Pu^{4+}) = (0.58 \pm 0.01) \times 10^{-5}$ cm^2/s $E_{\tau/4}$: Dependent on current density
	0.5 M H_2SO_4	Pt	Chronopot	25.8	$E_{\tau/4}$ = +0.51 [SCE]	Not quite reversible	64	$D(Pu^{4+}) = (0.50 \pm 0.01) \times 10^{-5}$ cm^2/s $E_{1/4}$: Dependent on current density
	2 M HNO_3	Pt	Sq vol		$E_{1/2}$ = +0.66 [SCE]	Not quite reversible	63	
Pu(IV) ← Pu(III)	0.5 M H_2SO_4	Pt	Chronopot	25.8	$E_{\tau/4}$ = +0.51 [SCE]	Reversible	64	$D(Pu^{3+}) = (0.47 \pm 0.01) \times 10^{-5}$ cm^2/s

DME, dropping mercury electrode; GC; glassy carbon electrode; DC pol, DC polarography; Radio pol, radio polarography; CTLC Coulo, coulometry at a cylindrical thin-layer cell; Chronopot, chronopotentiometry; CV, cyclic voltammetry; Sq vol, square-wave voltammetry; $E_{1/2}$, half-wave potential; E_{pc}, cathodic peak potential; E_{pa}, anodic peak potential; $E_{\tau/4}$, quarter-wave potential; SCE, saturated calomel electrode; MSE, mercury/mercurous sulphate (1 M H_2SO_4) electrode; SSE, silver–silver chloride electrode; D(M), diffusion constant of M; μ, ionic strength.

the disproportionation. The rate law at 25 °C is given by

$$-\mathrm{d}[UO_2^+]/\mathrm{d}t = k a_{H^+}[UO_2^+]^2 \quad (9)$$

where $k = 130$ (mole/dm^3)$^{-1}$/s at 25 °C in perchlorate solutions of $\mu = 0.4$. This result was further confirmed by other authors [22], but an anomaly was observed in strongly acidic chloride and perchlorate solutions [42]. The $ka_{H^+}^{-1}$ was found to be 6.500 ± 1.000 (mole/dm^3)$^{-2}$/s in sulphate solution (0.5 M $K_2SO_4 + 0.5$ M H_2SO_4) [43].

The mechanism of disproportionation of UO_2^+ was proposed as Eqn 10 [40], the sequence of Eqns 11 to 13 [41,44] or the combination of Eqns 11 and 14 [45].

$$2UO_2^+ + H^+ \rightleftharpoons UO_2^{2+} + UOOH^+ \quad (10)$$

$$UO_2^+ + H^+ \rightleftharpoons UOOH^+ \quad (11)$$

$$UO_2^+ + UOOH^{2+} \rightarrow UO_2^{2+} + UOOH^+ \text{(slow step)} \quad (12)$$

$$UOOH^+ \rightarrow \text{stable U(IV) species} \quad (13)$$

$$UO_2^+ + UOOH^{2+} \rightarrow HOUO_2^+ + UO^{2+} \text{ (slow step)} \quad (14)$$

$$UO^{2+} \rightarrow \text{stable U(IV) species} \quad (15)$$

With respect to the U(IV)/U(III) couple, Harris & Kolthoff [38,40] observed the polarogram for reduction of uranous sulphate in perchloric or hydrochloric acid, and confirmed that $E_{1/2}$ for this wave was the same as that for the 2nd wave of uranyl chloride. Therefore, it was supposed that the initial reaction was probably that of Eqn 7 or 8 followed by reaction of UO^+ or UOOH with hydrogen ion to result in U^{3+}. They concluded that the reduction wave of U(IV) at DME was irreversible, in accord with Heal [39]. Kitchevsky & Hindman [27] demonstrated, however, that the U(IV)/U(III) couple behaved reversibly at DME. They proposed the reaction of Eqn 16 on the basis of the experimental result that the reaction was independent of the hydrogen ion concentration.

$$U^{4+} + e \rightleftharpoons U^{3+} \quad (16)$$

The $E^{\circ\prime}$ of this reaction were determined as -0.631 ± 0.005 V vs. NHE in 1 M $HClO_4$ and -0.640 ± 0.005 V vs. NHE in 1 M HCl. The $E_{1/2}$ of the reversible wave shifted to more positive values with increasing acidity of rather dilute perchloric acid from 0.01 to 0.1 M [27]. The shift can be explained by considering that the hydrolysis of U(IV) may proceed in weakly acidic medium and that the predominant species of U(IV) may be UOH^{3+} up to about 0.1 M hydrogen ion. If UOH^{3+} is reduced to U^{3+} according to Eqn 17, the $E_{1/2}$ should shift to a more positive value by 59 mV per 10-fold increase in the hydrogen ion concentration.

$$UOH^{3+} + H^+ + e \rightarrow U^{3+} + H_2O \quad (17)$$

The $E_{1/2}$ becomes virtually constant and equal to -0.631 ± 0.005 V vs. NHE in the perchloric acid solutions of concentration higher than 0.1 M, which is expected from the hydrolysis constant of the U^{4+} cation.

An incompletely developed anodic wave at -0.19 V vs. SCE was observed in very weakly acidic solution containing U(IV) (0.001 M HCl + 0.1 M KCl) [27]. The wave was attributed to the oxidation of UOH^{3+} to UO_2^+.

As described above, the effect of ionic strength on the polarographic wave of UO_2^{2+}/UO_2^+ couple was investigated systematically in perchlorate solutions by Riglet *et al*. [1] in order to determine E° for the couple at $\mu = 0$. It was confirmed that the wave is reversible in the 0.5–3 M perchlorate solutions.

The polarographic reduction of UO_2^{2+} in nitric acid solution was found to be of one-electron mechanism at low acid (0.1 M) concentration and two-electron mechanism at high (2 M) acid concentration [46]. The reduction was concluded to be that of $UO_2NO_3^+$ to UO_2NO_3, since the $E_{1/2}$ was independent of c_{H^+}. The addition of methanol shifted negatively the $E_{1/2}$-value for the reduction of U(VI).

Reduction of either uranyl or uranous ion at DME, catalyzed by the reduction of nitrate ion [47], was utilized for the determination of traces of uranium [38].

All polarographic waves of uranium, except the oxidation wave of U(III) to U(IV) and the reduction wave of U(III) reported by Heal [48], were observed at the DME by McEwen & de Vries [29] in a sulfanilic acid solution, which is about the only buffer solution of a pH range from 3 to 4 which does not significantly complex uranium at any of the oxidation states (cf. Figure 1). Waves *A* and *G* in Fig. 1 represent the oxidation of mercury and reduction of hydrogen ions, respectively. Curve *H* represents the residual current of the supporting electrolyte. A slope of a plot of logarithmic analysis for wave *B* corresponding to oxidation of U(IV) was 40 mV, in poor agreement with the theoretical value of 59 or 30 mV for a one- or two-electrons reversible reaction, though the proximity of wave *C* made analysis of wave *B* difficult. A slope for wave *C* corresponding to oxidation of U(V) to U(VI) and wave *D* for reduction of U(VI) to U(V) was 60 mV, in good agreement with the theoretical value for a one-electron reversible reaction. Slope values of 70 and 90 mV were found for wave *E* for reduction of U(V) and wave *F* for reduction of U(IV) to U(III), respectively, indicating some irreversible character of these two reduction steps. Wave *E* was confirmed to be due to an irreversible reaction in accordance with previous works [27,38,39]. The irreversibility of wave *F* was attributed to the hydrolysis of U(IV) [27]. The $E_{1/2}$-value for wave *B* shifted negatively by 120 mV per one pH unit, suggesting that the ratio of the number of protons to that of electrons is 2 in the oxidation of U(IV).

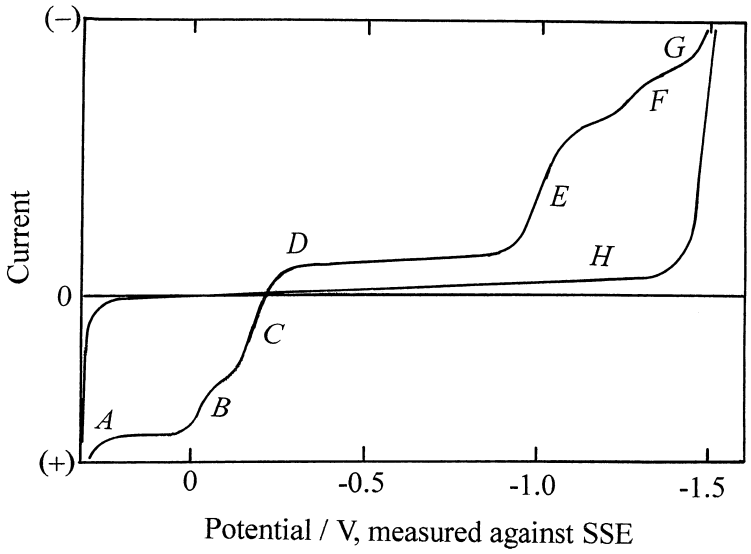

Fig. 1 Polarograms of uranium in a solution containing 0.1 M $NaClO_4$ and 0.1 M sulfanilate buffer (pH 3.1). The uranium reagent was uranous perchlorate containing some uranyl perchlorate. (A) Oxidation of mercury; (B) oxidation of U(IV) ; (C) oxidation of U(V) to U(VI); (D) reduction of U(VI) to U(V); (E) reduction of U(V); (F) reduction of U(IV) to U(III); (G) reduction of hydrogen ions; (H) residual current of the supporting electrolyte.

The redox reactions of uranium have also been investigated voltammetrically at electrodes other than DME, though sufficient data are not available. Only one reduction wave for UO_2^{2+} was observed at the gold and gold amalgam electrodes in acidic solution [49]. The gold amalgam electrode behaved like the gold electrode, though the current was observed at more negative potentials at the amalgam electrode.

Infrared spectro-electrochemical studies on the reduction of U(VI) at a platinum electrode by Best *et al.* [50] demonstrated that UO_2^{2+} and $(UO_2)_2(OH)_2^{2+}$ were present in a solution of pH near 3 before the electrolysis. On scanning the electrode potential to −0.2 V vs. SCE, the U(V) species, presumably UO_2^{+} either in the solution or in the solid phase attached to the electrode surface. Switching the potential to more negative values where the major reduction process at platinum was observed led to the diminishing of absorption bands of UO_2^{2+} and $(UO_2)_2(OH)_2^{2+}$ until they completely disappeared at −0.6 V vs. SCE.

A general increase in absorption at wave numbers below 900 cm^{-1}, at more negative potentials than −1 V vs. SCE, was speculated to be due to the decomposition of the solid phase of uranium oxide (most likely UO_2). Reversal of the potential scan direction showed all the reactions to be electrochemically irreversible.

The behavior of UO_2^{2+} at a graphite electrode in mildly acidic to neutral solutions containing magnesium chloride was investigated by cyclic voltammetry [51]. It was confirmed that the reduction mechanism of UO_2^{2+} was more simple than that reported for other electrodes, irrespective by whether the solution-soluble or surface-attached species were being examined.

The electrochemical reduction of UO_2^{2+} in 0.1–9 M H_3PO_4 was investigated by polarography, cyclic voltammetry, chronopotentiometry and controlled-potential coulometry [52]. In phosphoric acid solutions concentrated up to 1 M, an adsorption prewave appeared in addition to the main wave of the diffusion controlled one-electron transfer. The electrode reaction was mostly quasireversible, but it evolved according to the variation of UO_2^{2+} and acid concentrations, i.e. when the concentration of the UO_2^{2+} increased and/or that of phosphoric acid decreased, the redox reaction became reversible.

3.2 Neptunium

The Np(IV)/Np(III) couple has been investigated at DME in perchloric [53], hydrochloric [53,54] and sulphuric [30,55] acids. The $E_{1/2}$ for a chloride solution ($E^{\circ\prime} = +0.142 \pm 0.005$ V vs. NHE in 1 M HCl) satisfied the criteria of reversibility, but polarograms of Np(IV) in perchloric acid were not always symmetrical about the $E_{1/2}$. In the presence of perchloric acid, the $E_{1/2}$-values were by 30–40 mV more negative for pure Np(IV) than those for mixtures of Np(IV) and Np(III) [53]. Therefore, the Np(IV)/Np(III) couple was concluded to be not completely reversible. This irreversible feature was attributed to the difference in the number of water molecules co-ordinated to Np^{4+} and Np^{3+}. In the presence of chloride ions, the redox reaction was reversible, which was explained by considering the presence of a chloro-complex instead of a hydrated ion. In sulphate solutions, the $E_{1/2}$-value was highly dependent on the HSO_4^- concentration. The existence of $NpSO_4^{2+}$ and $Np(SO_4)_2$ was confirmed, while stable sulphate complexes of Np(III) were not found. The stability constant of $Np(SO_4)_2$ was determined to be 4360 [55].

The Np(IV)/Np(III) couple has also been studied in hydrochloric, nitric and perchloric acid solutions by AC polarography at DME [56,57]. In all cases, the peak potential of AC polarogram was equal to $E_{1/2}$ of DC polarogram, and the peak width at half peak height was 90 mV, as expected for a one-electron reversible reaction.

The redox process of the NpO_2^{2+}/NpO_2^{+} couple in perchloric acid solution was studied by cyclic voltammetry at a glassy carbon electrode by Plock [58]. He confirmed the redox process was to be reversible. Casadio & Orlandini investigated the couple by cyclic voltammetry at a pyrolytic graphite electrode [59].

Niese & Vecernik characterized the charge transfer of Np^{4+}, NpO_2^{+} and NpO_2^{2+} in perchloric, nitric and sulphuric acids by cyclic voltammetry at a glassy carbon electrode [60]. They observed one one-electron reduction wave of NpO_2^{2+} in perchloric or nitric acid solution instead of three one-electron reduction waves which had been observed at the pyrolytic graphite electrode in nitric acid solution by Casadio & Orlandini [59]. Though the redox reaction of the NpO_2^{2+}/NpO_2^{+} couple was not influenced by the coexistence of Np^{4+} in perchloric or nitric acid solution, an interaction between NpO_2^{2+} and Np^{4+} producing NpO_2^{+} was observed for sulphuric acid solution.

Propst [30] used a cylindrical cell with a conducting glass (antimony-doped tin oxide) electrode for coulometry in a thin layer of solution, and recorded current-potential curves of the reduction of Np(VI) to Np(III), the reduction of Np(IV) to Np(III), the oxidation of Np(IV) to Np(VI) and the oxidation of Np(V) to Np(VI) as shown in Fig. 2. Redox reactions of Np(VI)/Np(V) and Np(IV)/Np(III) couples were confirmed to be reversible, while the Np(V)/Np(IV) redox couple was extremely irreversible.

Riglet *et al*. [2] investigated redox reactions of the Np(VI)/Np(V) couple by voltammetry at a rotating platinum electrode or cyclic voltammetry at a stationary platinum electrode and the Np(IV)/Np(III) couple by cyclic voltammetry at a hanging mercury drop electrode in perchlorate solutions of various ionic strengths. They confirmed that the redox reaction of the NpO_2^{2+}/NpO_2^{+} couple is not quite reversible.

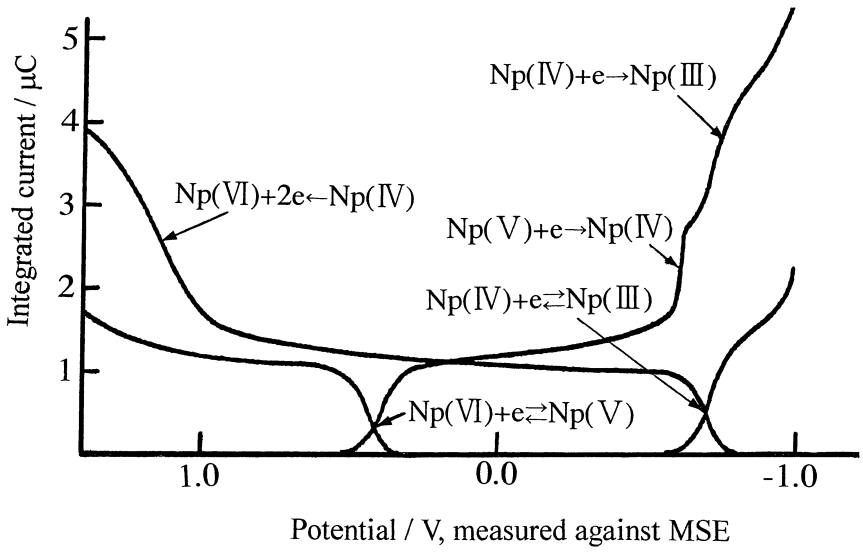

Fig. 2 Current–potential curves for the reduction of Np(VI) to Np(III), the reduction of Np(IV) to Np(III), the oxidation of Np(IV) to Np(VI) and the oxidation of Np(V) to Np(VI) measured by using a cylindrical cell with a conducting glass (antimony-doped tin oxide) electrode. MSE; mercuric sulphate electrode.

3.3 Plutonium

Polarography at DME has not been applied to plutonium ions in acidic aqueous solutions in the absence of special complexing agents.

Hindman [61] reported that the redox couple of the Pu(IV)/Pu(III) was reversible and independent of c_{H^+} above 0.3 M in perchloric acid solutions, and that Pu(IV) existed as the hydrated Pu^{4+}. Harvey *et al.* [62] studied the Pu(IV)/Pu(III) couple voltammetrically in perchloric, hydrochloric and sulphuric acids. Koyama [63] employed the square-wave voltammetry at a platinum electrode in order to investigate the reduction of Pu(IV) in hydrochloric and nitric acid solutions, and reported $E_{1/2}$ which agreed with accepted values.

Chronopotentiometry at a platinum electrode was applied for investigation of plutonium in acidic solutions [64]. For perchloric acid, a well-defined reversible wave was observed for the oxidation of Pu(III). For a sulphuric acid solution, one wave was observed in the chronopotentiogram for the oxidation of Pu(III) and another wave which was attributed to the formation of a platinum oxide film. The quarter-wave potential, $E_{\tau/4}$, did not depend on the current density for the reduction of Pu(IV) in perchloric or hydrochloric acid, but depended in nitric and sulphuric acids indicating that the reduction of Pu(IV) to Pu(III) proceeded somewhat less reversibly in these solutions. A well-defined wave was observed for the reduction of Pu(IV) in several acids. However, the interpretation of the results was difficult owing to the oxidation of the platinum electrode by Pu(IV). The reduction of Pu(VI) proceeds through two steps in perchloric acid, i.e. Pu(VI) to Pu(V) and Pu(V) to Pu(III). The $E_{\tau/4}$-value for both the 1st and the 2nd step of the reduction of Pu(VI) in perchloric acid depended on the current density. Hence, the two steps were considered to be irreversible. The diffusion coefficients of Pu(III), Pu(IV) and Pu(VI) in various acids were also given in this paper.

Cohen reported a set of current-potential curves for various plutonium ions in 1 M $HClO_4$ [31]. Though his potential measurement was not very precise since this work aimed at the preparation of a plutonium ion of the desired oxidation state, the result indicated that both redox processes of the Pu^{4+}/Pu^{3+} and the PuO_2^{2+}/PuO_2^{+} couples were almost reversible, while that of PuO_2^{2+}/Pu^{4+} couple was irreversible.

Riglet *et al.* [2] investigated redox reactions of Pu(VI)/Pu(V) and Pu(IV)/Pu(III) by cyclic voltammetry at a stationary platinum electrode in perchlorate media of various ionic strengths, and confirmed that these redox reactions were reversible.

3.4 Disproportionation of NpO_2^+, PuO_2^+, Np^{4+} and Pu^{4+}

The reduction currents of NpO_2^{2+} and PuO_2^{2+} or the oxidation currents of Np^{3+} and Pu^{3+} larger than those for one-electron reductions or one-electron oxidations have not been observed by ordinary voltammetric techniques in acidic solutions in the absence of certain formation of complexes. This fact suggests that the disproportionations of NpO_2^+, PuO_2^+, Np^{4+} and Pu^{4+} are not significant in aqueous acidic solutions unless, otherwise, the acid concentration is very high, in accordance with the results obtained by potentiometry and coulometry [65].

3.5 Reduction of MO_2^+ and reduction intermediates

Though reduction of MO_2^+ is expressed generally by Eqn 18 describing the electrochemical equilibrium, the reduction is considered to be a multistep reaction.

$$MO_2^+ + 4H^+ + 2e \rightarrow M^{3+} + 2H_2O \quad (18)$$

As described above, polarographic studies on the reduction or disproportionation of UO_2^+ indicated UO^{2+}, $UOOH^+$ or UOH^{3+} as the primary reduction products of UO_2^+.

The presence of PuO^{2+} as the intermediate species was also confirmed in the reduction of PuO_2^+ to Pu^{3+} based on the analysis of the voltammogram at the glassy carbon, GC, disk electrode in phosphate solutions [34,35].

Voltammograms for Pu ions in a mixed 1 M HNO_3 and 1.4 M H_3PO_4 solution observed at the GC electrode are presented in Fig. 3. Though two reduction peaks were observed in the voltammogram for the reduction of PuO_2^{2+} at the stationary electrode (curve 1), three waves appeared when the disk electrode was rotated (curves 2–5). The limiting currents, i_l, for these three waves were almost identical with each other when the rotation rate, ω, was as large as 1500 r.p.m., indicating a three-step reduction of PuO_2^{2+}, i.e. $PuO_2^{2+} \rightarrow PuO_2^+ \rightarrow$ Pu(IV) $\rightarrow$ Pu(III). The 1st wave is concluded to be due to a reversible one-electron reduction of PuO_2^{2+} to PuO_2^+ based on a slope of 58 ± 2 mV of logarithmic analysis, the i_l was proportional to $\omega^{1/2}$ and the $E_{1/2}$ was independent of the activity of H^+. Slopes of the logarithmic analysis for the 2nd and 3rd waves were about 90 and 95 mV, respectively, and i_l for these waves were not proportional to $\omega^{1/2}$. This result indicates that both waves are different from those of reversible processes controlled by diffusion. The ratio of i_l of the 2nd wave to that of the 3rd wave increased with the decrease of ω. The $E_{1/2}$-value for the 3rd wave, corresponding the reduction of Pu(IV) to Pu(III), was by ≈ 0.4 V more negative than that for the wave due to the reversible reduction of Pu^{4+} measured at the rotating GC disk electrode in the same solution (curve 6 in Fig. 3). This result suggests that the species of Pu(IV) produced during the reduction of PuO_2^{2+} is different from Pu^{4+}. Here, Pu^{4+} used to record curve 6 was the one-electron oxidation product of Pu^{3+} which had been prepared by dissolving a Pu metal with H_3PO_4. The plutonium species thus obtained were confirmed to be Pu^{3+} and Pu^{4+}. This assignment was based on the reversible characteristics of voltammograms for the one-electron reduction of the Pu(IV) (curve 6 in Fig. 3) and one-electron oxidation of Pu(III) (curve 7 in Fig. 3). Moreover, these voltammograms were independent of the H^+ activity, a_{H^+}, and $E_{1/2}$s of both voltammograms were the same.

The $E_{1/2}$s for the 2nd and 3rd waves of curve 4 in Fig. 3 were strongly dependent on the solution composition, as shown in Table 11. The $E_{1/2}$-values for these waves in solution nos 5 and 6 are much more negative than those in solution nos 1 to 4. Considering that differences between activity of $H_2PO_4^-$ in solution nos 1 and 6 and those of HPO_4^{2-} in solution nos 3 and 5 are not large but the difference in a_{H^+} is remarkable. We attribute the effect of the media on $E_{1/2}$s to the difference in the a_{H^+} values. The electrode processes for the 2nd and the 3rd waves may involve 2 H^+, as inferred taking into account that $E_{1/2}$s for the 2nd and the 3rd wave shifted negatively by ≈ 0.22 and 0.23 V with the a_{H^+} decrease by an order of magnitude and the slopes of logarithmic analyses of these waves were 90 and 95 mV, respectively.

Summarizing the results for the phosphate solutions discussed above, we may reasonably conclude that the voltammograms recorded at the rotating GC electrode at fairly high rotation rates correspond to the following electrode processes.

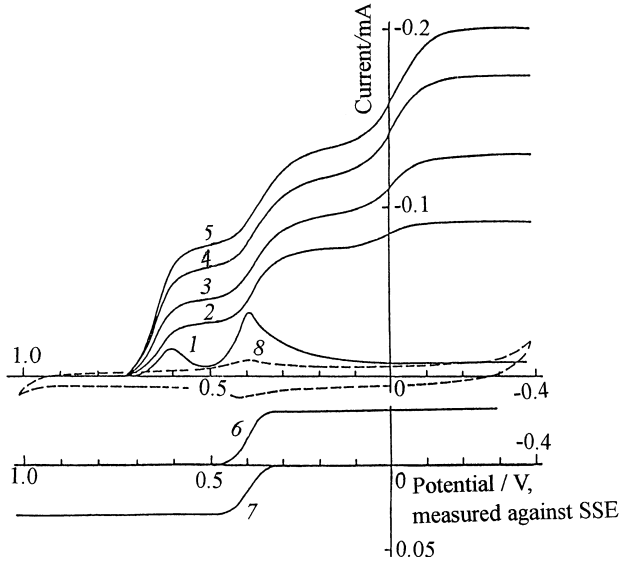

Fig. 3 Voltammograms for plutonium in a mixed 1 M HNO_3 and 1.4 M H_3PO_4 solution recorded at the glassy carbon disk electrode. (Curves 1–5) Reduction of PuO_2^{2+}; (curve 6) reduction of Pu^{4+}; (curve 7) oxidation of Pu^{3+}; (curve 8) residual current. Rotating rate of the disk electrode: (curve 1) 0; (curves 2, 6, 7 and 8) 250 r.p.m.; (curve 3) 500 r.p.m.; (curve 4) 1000 r.p.m.; (curve 5) 1500 r.p.m.

Table 11 Half-wave potentials* determined from voltammograms for plutonium ions† in the mixed phosphate-nitrate solutions

	Solution	Half–wave potential (V vs. SSE)							
		Reduction of PuO_2^{2+}			Reduction of Pu^{4+}	Oxidation of Pu^{3+}	Activities of ionic species (M)‡		
		1st wave	2nd wave	3rd wave			H^+	$H_2PO_4^-$	HPO_4^{2-}
(1)	0.70 M H_3PO_4 + 1.0 M HNO_3	+0.67	+0.35	−0.02	+0.45	+0.45	0.77	7.2×10^{-3}	5.9×10^{-10}
(2)	1.4 M H_3PO_4 + 1.0 M HNO_3	+0.65	+0.36	−0.01	+0.42	+0.42	0.80	1.4×10^{-2}	1.1×10^{-9}
(3)	2.0 M H_3PO_4 + 1.0 M HNO_3	+0.65	+0.37	−0.02	+0.40	+0.40	0.83	1.9×10^{-2}	1.5×10^{-9}
(4)	3.0 M H_3PO_4 + 1.0 M HNO_3	+0.64	+0.37	−0.02	+0.38	+0.38	0.88	2.7×10^{-2}	1.9×10^{-9}
(5)	0.125 M H_3PO_4 + 0.3 M HNO_3 + 0.7 M $NaNO_3$	+0.69	+0.23	−0.16	+0.42	+0.42	0.21	4.8×10^{-3}	1.5×10^{-9}
(6)	0.25 M H_3PO_4 + 0.4 M HNO_3 + 0.6 M $NaNO_3$	+0.67	+0.26	−0.12	+0.42	+0.42	0.28	6.8×10^{-3}	1.5×10^{-9}

* Measured at a rotating glassy carbon disk electrode (rotating rate $\omega = 1000$ r.p.m., potential scan rate $v = 5$ mV/s).
† Concentration of plutonium ions: 1.12×10^{-3} M.
‡ Calculated on the basis of $pK_{a1} = 2.1$; $pK_{a2} = 7.2$; $pK_{a3} = 12.1$.

The 1st wave:

$$PuO_2^{2+} + e \rightarrow PuO_2^{+} \quad (19)$$

The 2nd wave:

$$PuO_2^{+} + 2H^{+} + e \rightarrow PuO^{2+} + H_2O \quad (20)$$

The 3rd wave:

$$PuO^{2+} + 2H^{+} + e \rightarrow Pu^{3+} + H_2O \quad (21)$$

The participation of PuO^{2+} as a Pu(IV) species is also supported by the irreversible nature of the 3rd wave which was observed in a much more negative potential range than that for the reduction of Pu^{4+} to Pu^{3+}. Here, the electrode process accompanied by the breaking of the metal-oxygen bond is usually irreversible and requires a large overpotential.

The PuO^{2+} species is unstable and decomposes into Pu^{4+} through the reaction of Eqn 22, which explains that, with lowering of ω, the 2nd wave increased and the 3rd wave decreased instead, and the reversibility of the electrode reaction for the 2nd wave increased, as indicated by the slope of the logarithmic analysis of the wave. A slight positive shift of $E_{1/2}$ of the 2nd wave with lowering of ω is also attributable to reaction of Eqn 22, since the reversible reduction of Pu^{4+} to Pu^{3+} takes place at more positive potentials than the potentials for Eqn 20.

$$PuO^{2+} + 2H^{+} \rightleftharpoons Pu^{4+} + H_2O \quad (22)$$

The chemical reaction (22) that follows the electrode process (20) is pronounced at the stationary electrode, as the resident time of PuO^{2+} at the electrode surface is longer than that at the rotating electrode. Therefore, the reduction wave of PuO_2^{+} at the stationary electrode appears as a two-electron reduction peak.

Taking into account that the two-step reduction of PuO_2^{+} was not observed in nitric acid solutions in the absence of phosphate ions, we consider the role of the phosphoric acid in the reduction of PuO_2^{+} to be the stabilization of PuO^{2+} by complex formation between PuO^{2+} and the phosphate anions.

The disproportionation of PuO^{2+}, such as Eqn 23, is an alternative to the reaction which explains the growth of the 2nd wave in compensation for the decrease of the 3rd wave, the enhancement of the reversibility of the 2nd wave and the slight positive shift of $E_{1/2}$ of the 2nd wave with lowering ω. The disproportionation is discussed below (Section 4.2).

$$2PuO^{2+} \rightleftharpoons PuO_2^{+} + Pu^{3+} \quad (23)$$

Such M(IV) species combined with oxygen as PuO^{2+} was proposed also for the U(IV) species produced by the reduction of UO_2^{+} at the column electrode in weakly acidic chloride solutions such as the mixture of 0.1 M HCl and 0.1 M KCl [32] or by the disproportionation of UO_2^{+} investigated polarographically [40,41,44,45,48].

Though the reduction of NpO_2^{+} could not be observed at the rotating GC disc electrode in phosphate solutions because of the disturbance due to the hydrogen evolution, the results obtained by flow coulometry predicted the presence of NpO^{2+} as intermediate in the reduction of NpO_2^{+} to Np^{4+} or Np^{3+} (cf. section 4.1).

4 REDOX REACTIONS OF URANIUM, NEPTUNIUM AND PLUTONIUM IN ACIDIC AQUEOUS SOLUTIONS INVESTIGATED BY FLOW COULOMETRY

A quantitative electrolysis can be achieved very rapidly (e.g. within 10 s) with small over-voltage by using a column electrode, even if the electrode reaction is totally irreversible (cf. Appendix and Fig. 4), since surface area of the working electrode of the column electrode is very large as for the solution volume in the column. Because of this unmatched advantage, the electrolysis with the column electrode in a flow system, which is called flow coulometry, is very useful for preparation of ions of the desired oxidation state as well as the rapid determination or collection of various metals [34,66,67]. This technique is especially favorable for the preparation of unstable species for the subsequent investigation

of their redox processes. The current-potential curve observed by flow coulometry is called coulopotentiogram.

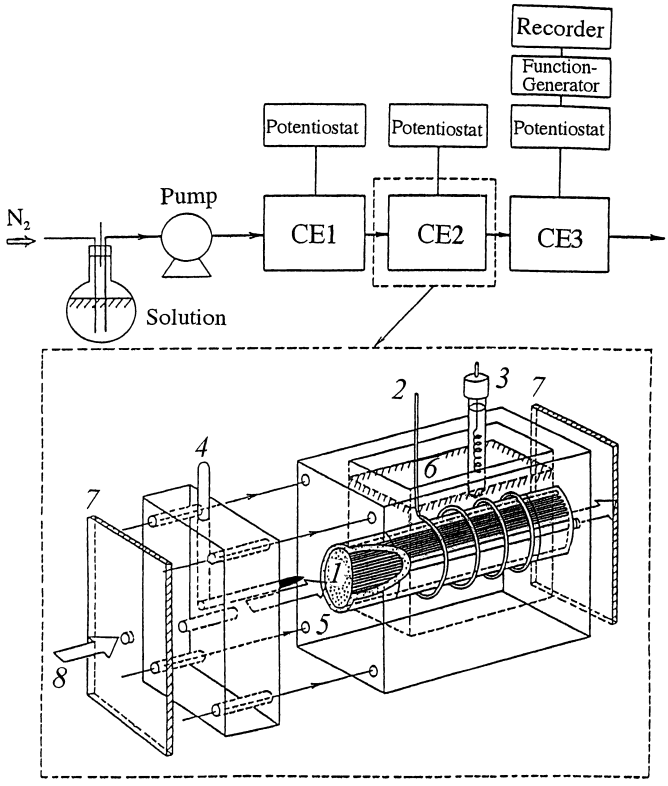

Fig. 4 Block diagram of the flow electrolysis system (top) and scheme of column electrode (bottom). (1) Working electrode of glassy carbon fibers; (2) Pt counter electrode; (3) reference electrode (SSE); (4) contact for working electrode; (5) electrolytic diaphragm; (6) compartment of counter electrode; (7) Neoprene seal; (8) sample solution.

4.1 Electrode processes of the uranium, neptunium and plutonium cations investigated by flow coulometry at the column electrode

Flow coulometry has been applied by the authors in order to elucidate the overall redox behavior of the actinide ions (M: U, Np or Pu) in perchloric acid, nitric acid, hydrochloric acid, sulphuric acid and mixtures of phosphoric acid and nitric acid [32–35,68]. Coulopotentiograms of M were measured by using the multistep column electrodes, in which 2 or 3 column electrodes were connected in series. The coulopotentiograms are presented in Figs 5–8 after correction for the residual currents of which one example is shown by the dotted line in Fig. 5. In these figures, the number of electrons involved in the redox reaction, n, converted from the current based on Eqn A1 in the Appendix is plotted on the ordinate instead of the current. In connection with the measurement, though flow coulometry has unique and unmatched advantages as mentioned above, the potential measured by this method is not very precise (± 0.01 V) compared with that in polarography or voltammetry, because of the complicated configuration of the column electrode with the working electrode of an extremely large surface area.

Curves 1(U) in Figs 5–7 are coulopotentiograms for the reduction of UO_2^{2+} in nitric, perchloric and sulphuric acid solutions, respectively, which were recorded at the 1st column (CE1) of the system composed of two-step column electrodes by forcing a solution containing UO_2^{2+} into the system at a constant flow rate, f, and scanning the potential applied to the working electrode at a constant rate, ν. A silver/silver chloride electrode with saturated KCl, SSE, was employed as the reference electrode. The limiting currents of curves 1(U) suggested that these curves corresponded to two-electron reduction of

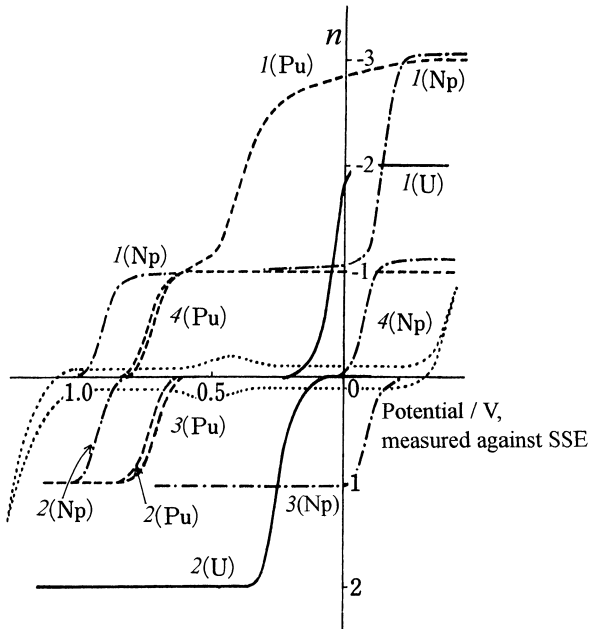

Fig. 5 Coulopotentiograms for the uranium, neptunium and plutonium ions in 1 M HNO_3. Reduction of UO_2^{2+}, NpO_2^{2+} or PuO_2^{2+} – curve 1(U), 1(Np) or 1(Pu); oxidation of U(IV), Np(V) or Pu(V) – curve 2(U), 2(Np) or 2(Pu); oxidation of Np(III) or Pu(III) – curve 3(Np) or 3(Pu); reduction of Np(IV) or Pu(IV) – curve 4(Np) or 4(Pu); residual current – dotted line. Sample concentration 10^{-3} M. Flow rate 1.5 mL/min. Scan rate 0.2 mV/s.

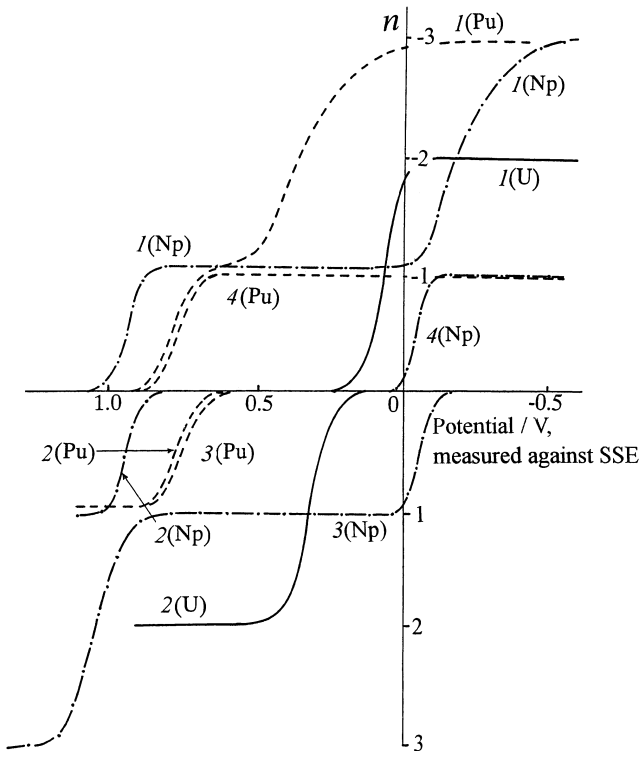

Fig. 6 Coulopotentiograms for the uranium, neptunium and plutonium ions in 1 M $HClO_4$. Reduction of UO_2^{2+}, NpO_2^{2+} or PuO_2^{2+} – curve 1(U), 1(Np) or 1(Pu); oxidation of U(IV), Np(V) or Pu(V) – curve 2(U), 2(Np) or 2(Pu); oxidation of Np(III) or Pu(III) – curve 3(Np) or 3(Pu); reduction of Np(IV) or Pu(IV) – curve 4(Np) or 4(Pu). Sample concentration 10^{-3} M. Flow rate 1.5 mL/min. Scan rate 0.2 mV/s.

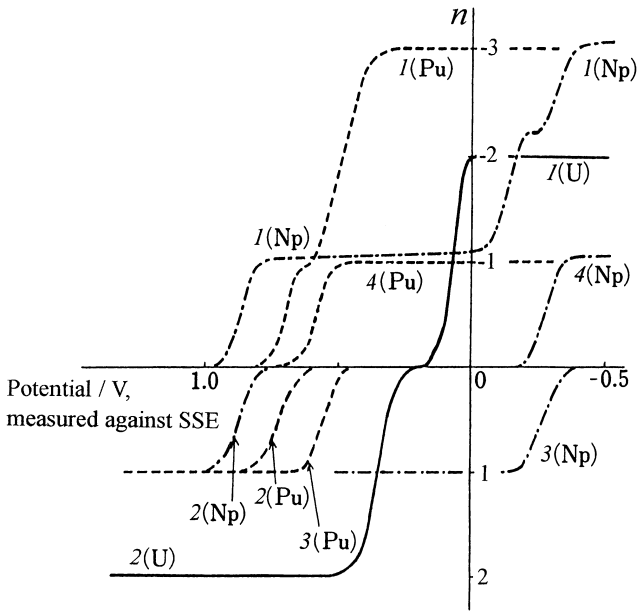

Fig. 7 Coulopotentiograms for the uranium, neptunium and plutonium ions in 0.5 M H_2SO_4. Reduction of UO_2^{2+}, NpO_2^{2+} or PuO_2^{2+} – curve 1(U), 1(Np) or 1(Pu); oxidation of U(IV), Np(V) or Pu(V) – curve 2(U), 2(Np) or 2(Pu); oxidation of Np(III) or Pu(III) – curve 3(Np) or 3(Pu); reduction of Np(IV) or Pu(IV) – curve 4(Np) or 4(Pu); residual current – curve 5. Sample concentration 10^{-3} M. Flow rate 1.5 mL/min. Scan rate 0.2 mV/s.

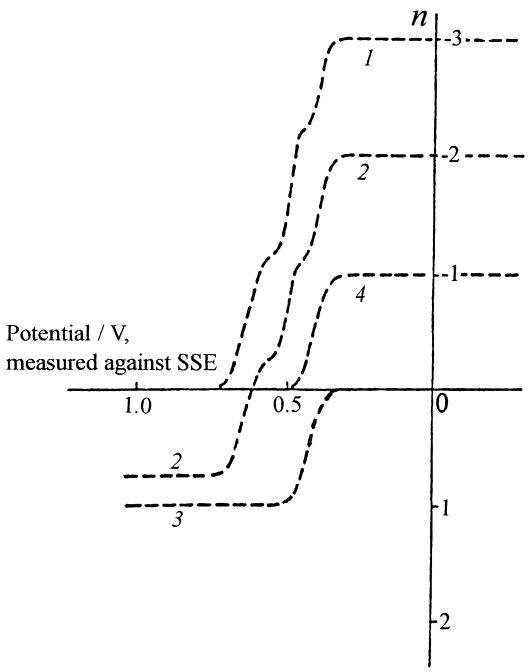

Fig. 8 Coulopotentiograms for the plutonium ions in a mixed 1 M HNO_3 and 1.4 M H_3PO_4 solution. (curve 1) Reduction of PuO_2^{2+}; (curve 2) oxidation-reduction of Pu(V); (curve 3) oxidation of Pu(III) ; (curve 4) reduction of Pu(IV). Sample concentration 10^{-3} M. Flow rate 1.5 mL/min. Scan rate 0.2 mV/s.

UO_2^{2+} to U(IV) in all solutions investigated. The further reduction could not be observed due to the hydrogen evolution.

Curves 2(U) in Figs 5–7 were recorded at the 2nd column (CE2) of the system composed of the two-step column electrodes by introducing the reduction product of UO_2^{2+} at CE1, i.e. U(IV), obtained at a potential in the range available for the limiting currents in curves 1(U). The limiting currents in curves 2(U) suggested a two-electron oxidation of U(IV). The oxidation waves appeared at potentials much more positive than those for the reduction of UO_2^{2+}. This behavior indicated that the redox process between UO_2^{2+} and U(IV) is irreversible in all solutions investigated. The results of theoretical analysis of the coulopotentiograms according to Eqns A3 and A5 in Appendix also supported the irreversible nature of the studied processes.

Coulopotentiograms identical with curves 2(U) in Figs 5–7 were obtained when they were recorded after introducing U^{4+} into the column electrode. Here, U^{4+} was prepared by dissolution of the uranium metal with $HClO_4$ followed by purging air through the resulted solution [69]. Therefore, it is reasonable to conclude that U(IV) produced by the reduction of UO_2^{2+} at CE1 is U^{4+}.

General aspects of the reduction behavior of NpO_2^{2+} and PuO_2^{2+} are similar to each other. A one-electron wave for the reduction of MO_2^{2+} to M(V) (M: Np or Pu) and a two-electron wave for the further reduction of M(V) to M(III) were observed in coulopotentiograms for nitric and perchloric acids, as shown by curves 1(Np) and 1(Pu) in Figs 5 and 6. The dependencies of $E_{1/2}$s on f and the logarithmic analyses of the coulopotentiograms suggested that the process of the one-electron reduction of MO_2^{2+} was reversible and that of the two-electron reduction of M(V) was irreversible.

The oxidation of M(V) was investigated by introducing the ion prepared at CE1 into CE2 as shown by curves 2(Np) and 2(Pu) in Figs 5–7. The $E_{1/2}$-value for the oxidation of M(V) was almost the same as that for the reduction of MO_2^{2+}. This agreement of the $E_{1/2}$-values and the results of the logarithmic analyses of the oxidation waves confirmed that the redox process of MO_2^{2+}/M(V) was reversible.

The oxidation of M(III) was investigated by introducing the three-electron reduction product of MO_2^{2+} at CE1 into CE2 as shown by curve 3(Np) or 3(Pu) in Figs 5–7. The waves corresponding to the one-electron oxidation of M(III) to M(IV) were reversible. Further oxidation, except that of Np in perchloric acid, could not be observed because of the large residual current due to the oxidation of the background electrolyte.

Coulopotentiograms identical with curves 3(Np) and 3(Pu) were obtained when they were recorded by introducing Np^{3+} and Pu^{3+}, respectively, into the column electrode. Here, Np^{3+} or Pu^{3+} was prepared by dissolving neptunium or plutonium metal with perchloric acid [70]. Hence, Np(III) or Pu(III) produced by the three-electron reduction of NpO_2^{2+} or PuO_2^{2+} at CE1 is attributable to Np^{3+} or Pu^{3+}, respectively.

The reduction of M(IV) which had been prepared by oxidizing M^{3+} at CE2 was investigated by using CE3 of the system consisting of the three-step column electrodes. The results are given by curves 4(Np) and 4(Pu). The one-electron reduction wave whose $E_{1/2}$ is identical with that for the oxidation of M^{3+} to M(IV) suggested the reversible M(IV)/M^{3+} process.

The effect of f on the coulopotentiogram was elucidated. The $E_{1/2}$s for redox processes of $NpO_2^{2+} \rightleftharpoons$ Np(V), Np(IV) $\rightleftharpoons Np^{3+}$, $PuO_2^{2+} \rightleftharpoons$ Pu(V) and Pu(IV) $\rightleftharpoons Pu^{3+}$, summarized in Table 12, are independent of f, which confirms the reversible nature of these processes. However, $E_{1/2}$ for processes of $UO_2^{2+} \rightarrow U^{4+}$, Np(V) $\rightarrow Np^{3+}$ and Pu(V) $\rightarrow Pu^{3+}$ depended strongly on f as listed in Table 13.

The effect of the hydrogen ion concentration, c_{H^+}, on the redox processes was examined in nitrate solutions by keeping the NO_3^- concentration constant, $c_{HNO_3} + c_{NaNO_3} = 2.0$ M. The $E_{1/2}$s for redox processes of $NpO_2^{2+} \rightleftharpoons$ Np(V), Np(IV) $\rightleftharpoons Np^{3+}$, $PuO_2^{2+} \rightleftharpoons$ Pu(V) and Pu(IV) $\rightleftharpoons Pu^{3+}$ (Table 12) were independent of c_{H+}, which indicates that bonds between M and oxygen are not formed or ruptured in these processes. Therefore, species indicated as Np(V), Np(IV), Pu(V) and Pu(IV) in the discussion above are considered to be NpO_2^+, Np^{4+}, PuO_2^+ and Pu^{4+}, respectively. The $E_{1/2}$s for redox processes of $UO_2^{2+} \rightarrow U^{4+}$, Np(V) $\rightarrow Np^{3+}$ and Pu(V) $\rightarrow Pu^{3+}$ varied with c_{H^+} as listed in Table 13, thus indicating the participation of the M-oxygen bonding in these processes.

Referring to the above described results, we can summarize reactions occurring at the column electrode as follows;

Table 12 Half–wave potentials of reversible coulopotentiograms for the Np and Pu ions in various solutions determined by flow coulometry

Electrode reaction	Solution	Half-wave potential (V vs. SSE)		
		Cathodic	Anodic	Mean
$NpO_2^{2+} \rightleftharpoons NpO_2^{+}$	1 M $HClO_4$	+0.94	+0.94	+0.94
	1 M HNO_3	+0.91	+0.91	+0.91
	0.5 M H_2SO_4	+0.87	+0.88	+0.88
$PuO_2^{2+} \rightleftharpoons PuO_2^{+}$	1 M $HClO_4$	+0.77	+0.78	+0.78
	1 M HNO_3	+0.74	+0.74	+0.74
	0.5 M H_2SO_4	+0.71	+0.73	+0.72
	1 M HNO_3 + 1.4 M H_3PO_4	+0.66	+0.66	+0.66
$Np^{4+} \rightleftharpoons Np^{3+}$	1 M $HClO_4$	−0.06	−0.06	−0.06
	1 M HNO_3	−0.13	−0.13	−0.13
	0.5 M H_2SO_4	−0.21	−0.21	−0.21
$Pu^{4+} \rightleftharpoons Pu^{3+}$	1 M $HClO_4$	+0.79	+0.76	+0.77
	1 M HNO_3	+0.73	+0.71	+0.72
	0.5 M H_2SO_4	+0.59	+0.57	+0.58
	1 M HNO_3 + 1.4 M H_3PO_4	+0.41	+0.43	+0.42

Table 13 Effect of the flow rate or hydrogen ion concentration of a sample solution on half-wave potentials of irreversible coulopotentiograms for the U, Np and Pu ions in nitric acid solutions

Electrode reaction	Flow rate (mL/min)	Hydrogen ion concentration (M)	Half-wave potential (V vs. SSE)
$UO_2^{2+} \rightarrow U(IV)$	0.5	1.0	+0.07
	1.5	1.0	+0.05
	3.0	1.0	+0.03
	1.5	0.2	+0.04
	1.5	2.0	+0.06
$U(IV) \rightarrow U(VI)$	0.5	1.0	+0.19
	1.5	1.0	+0.25
	3.0	1.0	+0.33
	1.5	0.2	+0.18
	1.5	2.0	+0.29
$NpO_2^{+} \rightarrow Np(III)$	0.5	1.0	−0.06
	1.5	1.0	−0.15
	3.0	1.0	−0.28
	1.5	0.2	−0.21
	1.5	2.0	−0.13
$PuO_2^{+} \rightarrow Pu(III)$	0.5	1.0	+0.46
	1.5	1.0	+0.37
	3.0	1.0	+0.25
	1.5	0.2	+0.25
	1.5	2.0	+0.39

Curve 1(U):

$$UO_2^{2+} + 4H^+ + 2e \rightarrow U^{4+} + 2H_2O \quad (24)$$

The 1st waves in curves 1(Np) and 1(Pu):

$$NpO_2^{2+} + e \rightarrow NpO_2^{+} \quad (25)$$

$$PuO_2^{2+} + e \rightarrow PuO_2^{+} \quad (26)$$

The 2nd wave in curves 1(Np) and 1(Pu):

$$NpO_2^{+} + 4H^{+} + 2e \rightarrow Np^{3+} + 2H_2O \quad (27)$$

$$PuO_2^{+} + 4H^{+} + 2e \rightarrow Pu^{3+} + 2H_2O \quad (28)$$

Curve 2(U):

$$U^{4+} + 2H_2O - 2e \rightarrow UO_2^{2+} + 4H^{+} \quad (29)$$

Curves 2(Np) and 2(Pu):

$$NpO_2^{+} - e \rightarrow NpO_2^{2+} \quad (30)$$

$$PuO_2^{+} - e \rightarrow PuO_2^{2+} \quad (31)$$

The 1st waves in curve 3(Np) and curve 3(Pu):

$$Np^{3+} - e \rightarrow Np^{4+} \quad (32)$$

$$Pu^{3+} - e \rightarrow Pu4 \quad (33)$$

Curves 4(Np) and 4(Pu):

$$Np^{4+} + e \rightarrow Np^{3+} \quad (34)$$

$$Pu^{4+} + e \rightarrow Pu^{3+} \quad (35)$$

Although the 2nd oxidation wave was not observed in curve 3(Np) recorded in nitrate media because of the oxidation of the solutions, the reaction for the further oxidation of Np^{4+} was estimated from the result obtained in perchlorate solutions, as Eqn 36.

The 2nd wave in curve 3(Np) in Fig. 6:

$$Np^{4+} + 2H_2O - 2e \rightarrow NpO_2^{2+} + 4H^{+} \quad (36)$$

Because irreversible processes among reactions of Eqns 24 to 36 involve breaking or formation of the M-oxygen bond which requires large activation energy, the electrode reduction of NpO_2^{+} to Np^{4+} or PuO_2^{+} to Pu^{4+} is considered to proceed at the potential more negative than that of Np^{4+} to Np^{3+}or Pu^{4+} to Pu^{3+}. Therefore, the reduction by the column electrolysis of NpO_2^{+} or PuO_2^{+} produces Np^{3+} or Pu^{3+}, respectively. Similarly, the oxidation of U^{4+} which involves the formation of U-oxygen bonding proceeds at the potential more positive than that for the oxidation of UO_2^{+} to UO_2^{2+}, and, hence, the column electrolysis of U^{4+} produces UO_2^{2+}.

For reversible processes of $NpO_2^{2+} \rightleftharpoons NpO_2^{+}$, $PuO_2^{2+} \rightleftharpoons PuO_2^{+}$, $Np^{4+} \rightleftharpoons Np^{3+}$ and $Pu^{4+} \rightleftharpoons Pu^{3+}$, the differences in $E_{1/2}$s observed for different acids (see Table 12) can be explained quantitatively by taking into account stability constants of complexes of the M ions with anions composing the acids. The $E_{1/2}$s in sulphate solutions were more negative than those in perchlorate, chloride or nitrate solutions, since stability constants of the sulphate complexes of NpO_2^{2+}, PuO_2^{2+}, Np^{4+} and Pu^{4+} are much larger than those of NpO_2^{+}, PuO_2^{+}, Np^{3+} and Pu^{3+}, respectively. The stability constants of complexes of M^{4+} (U^{4+}, Np^{4+} and Pu^{4+}) with sulphate are larger than those of the M ions of other oxidation states. Therefore, the reduction of MO_2^{+} to M^{4+} is facilitated and results in the positive shifts of $E_{1/2}$s of reduction waves of UO_2^{2+} to U^{4+} and PuO_2^{+} to Pu^{3+} as well as the splitting of the wave for the reduction of NpO_2^{+} to Np^{3+} into two waves. The oxidations of M^{4+} to MO_2^{2+} are depressed in sulphate solutions resulting in the positive shifts of $E_{1/2}$s of the oxidation waves.

Coulopotentiogram 1 in Fig. 8 for the reduction of PuO_2^{2+} in the phosphoric acid mixture consisted of three waves. The second wave is attributable to the one-electron reduction of PuO_2^{+} to PuO^{2+}, since PuO^{2+} is expected to be stabilized in the mixture due to the complex formation with phosphate species (cf. section 3.5). As the potentials where the second wave appeared depended on f, the reduction is considered to be irreversible. The $E_{1/2}$ in the coulopotentiogram for the irreversible reduction at the

column electrode generally appears at more positive potentials than the $E_{1/2}$ in the ordinary voltammogram, which explains that $E_{1/2}$ of the second wave of curve 1 in Fig. 8 was much more positive than that in the voltammogram in Fig. 3. The $E_{1/2}$-value of the third wave is identical to that for the reduction of Pu^{4+} to Pu^{3+}, which can be understood by considering that the resident time of the solution in the column electrode is long enough for the complete decomposition of the primary reduction product of PuO_2^+, PuO^{2+}, to Pu^{4+} (Eqn 22) in the column. Therefore, the overall reduction of PuO_2^{2+} in phosphate solutions at the column electrode is concluded to be

$$PuO_2^{2+} \rightarrow PuO_2^+ \rightarrow PuO^{2+}(\text{chemical decomposition to } Pu^{4+}) \rightarrow Pu^{3+} \quad (37)$$

A similar reduction mechanism was observed by flow coulometry for the reduction of NpO_2^{2+} in sulphuric acid solutions [cf. curve 1(Np) in Fig. 7]. Detailed analysis of the two-step reduction waves of NpO_2^+ leads to the assumption that such intermediate species as NpO^{2+}, instead of Np^{4+}, may take part in the reduction of NpO_2^+ [71], i.e. $NpO_2^+ \rightarrow NpO^{2+}$ (chemical decomposition to Np^{4+}) $\rightarrow Np^{3+}$.

4.2 Disproportionation of MO_2^+ during the electrolysis by flow coulometry

The number of electrons, n, involved in the first reduction wave of the polarograms of UO_2^{2+} observed at the DME in acidic perchlorate, chloride or nitrate solutions was between 1 and 2 due to the disproportionation of the one-electron reduction product of UO_2^{2+}, UO_2^+, as described previously. However, the n-value determined by the column electrolysis was 2, since the resident time of the solution on the electrode surface in the column electrode is much longer than that at the surface of DME, and the reduction of the disproportionation product, UO_2^{2+}, occurs successively during the resident time. Hence, the two-electron reduction of UO_2^{2+} observed by flow coulometry at the column electrode should be expressed by the combination of reactions of Eqns 5, 11 and 12 or Eqns 5, 11 and 14 followed by the chemical decomposition of $UOOH^+$ or UO^{2+} to U^{4+} rather than Eqn 24.

The shifts of $E_{1/2}$ of the two-electron reduction wave in the coulopotentiogram with c_{H^+} and f (cf. Table 13) are attributable to the dependence of the rate constant of the disproportionation reaction on c_{H^+} and the resident time of the solution on the electrode surface.

The one-electron reduction wave of NpO_2^{2+} or PuO_2^{2+} was observed even by the column electrolysis indicating that the disproportionation reactions of NpO_2^+ and PuO_2^+ are much slower than that of UO_2^+ [65,72].

4.3 Reduction mechanisms of MO_2^+ (M = Np or Pu) and reduction intermediates investigated by flow coulometry

The electrochemical characteristic of GC fiber electrode depends strongly on the condition under which the fiber was prepared, as well known, and fibers prepared in different years often have different characteristics even though they were commercially available as those of the same trade names. When GC fibers of different characteristics are used properly, more detailed features of electrode reactions might be elucidated.

Coulopotentiograms for the redox reactions of Np cations in 1 M $HClO_4$ are shown in Fig. 9. The working electrode material of the column electrode employed to record the coulopotentiograms was the GC fiber which was the same as that used to record coulopotentiograms in Fig. 6 in its trade name (GC-20, Tokai Carbon Co., Japan), but produced recently. The electron transfer at this GC fiber electrode was relatively slow compared with that at the GC fiber electrode used for Fig. 6, and, hence, the large overpotential was required to observe an irreversible electrode reaction, such as that involving the breaking or formation of the metal–oxygen bonds.

Two waves were observed in the coulopotentiogram for the reduction of NpO_2^+ recorded at the relatively high f (curve 1 in Fig. 9). This coulopotentiogram was recorded at CE2 by introducing the one-electron reduction product of NpO_2^{2+} prepared at CE1, NpO_2^+, into CE2. The two waves are attributable to the successive reductions of NpO_2^+, $NpO_2^+ \rightarrow Np(IV) \rightarrow Np(III)$, since limiting currents of both waves correspond to one-electron reduction ($n = 1$). When the one-electron reduction product of NpO_2^+ prepared at CE2 of -0.30 V vs. SSE, Np(IV), was introduced into CE3, and the oxidation behavior was

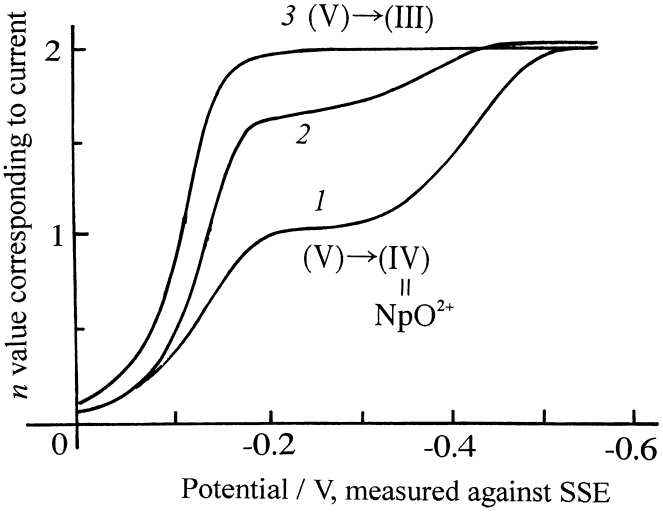

Fig. 9 Coulopotentiograms for reduction of 10^{-3} M NpO_2^+ in 1 M $HClO_4$. Flow rate: (curve 1) 0.52 mL/min; (curve 2) 0.35 mL/min; (curve 3) 0.16 mL/min. Scan rate 0.2 mV/s.

investigated at CE3, an oxidation wave was observed with $E_{1/2}$ of the same as that observed in the coulopotentiogram for the oxidation of Np^{3+} [curve 3(Np) in Fig. 6]. However, the magnitude of the limiting current corresponded to $n = 0.45$–0.48 indicating that the reduction product at CE2, Np(IV), was converted to Np^{3+} and Np(V) almost quantitatively by the disproportionation reaction of Eqn 38 before entering into CE3.

$$2Np(IV) \rightarrow Np^{3+} + Np(V) \tag{38}$$

The one-electron reduction product at CE2 of −0.30 V, Np(IV), is considered to be a different species from Np^{4+}, taking into account that the disproportionation of Np^{4+} has been confirmed to be slow [72]. The discussion on the species of U(IV) or Pu(IV) in sections 3.1 or 3.5 suggests that the possible species of Np(IV) is NpO^{2+}. That is, the reaction at potentials of the first wave of curve 1 in Fig. 9 might be

$$NpO_2^+ + 2H^+ + e \rightarrow NpO^{2+} + H_2O \tag{39}$$

The following consideration indicates that the Np(V) species, produced by reaction 38, is also different from the commonly accepted form, NpO_2^+. The limiting current of the first wave of coulopotentiogram 1 in Fig. 9 corresponded to $n = 1$. The current should be that of more than $n = 1.5$, however, if Np(V) is NpO_2^+, since NpO_2^+ can be reduced at –0.30 V and a half of Np(IV) must be converted to Np(V) by the quantitative reaction of Eqn 38. The species of Np(V) (which will be denoted by Np(V)*) has not been identified, yet.

The *n*-value for the limiting current of the 1st wave increased with the decrease of *f*, and *n* was 2 when *f* was sufficiently low as 0.16 mL/min (cf. curves 2 and 3 in Fig. 9). When *f* is low, the unstable Np(V)* produced in CE2 might be converted chemically into NpO_2^+ during its stay in CE2, and the current due to the reduction of NpO_2^+ might be added to the limiting current.

When the oxidation behavior of the two-electron reduction product prepared at CE2 of −0.55 V vs. SSE, Np(III), was investigated at CE3, an oxidation wave identical with curve 3(Np) in Fig. 6 for the oxidation of Np^{3+} to Np^{4+} was observed. The limiting current of the oxidation wave corresponded to $n = 1.0$ indicating that NpO_2^+ was reduced to Np^{3+} quantitatively at CE2 of –0.55 V.

The 2nd wave of curve 1 in Fig. 9 observed at high *f* can be explained by considering the two-electron reduction of the product of the disproportionation reaction 38, Np(V)*, of which concentration is half of that of NpO_2^+ introduced into CE2.

$$Np(V)^* + 2e \rightarrow Np^{3+} \tag{40}$$

That is, reactions at potentials of the 2nd wave correspond to the reduction of NpO_2^+ [Eqn 39] followed by the disproportionation [Eqn 38] and the reduction of Np(v)* [Eqn 40]. The 2nd wave shifted to more positive values with lowering f, indicating irreversible nature of the Np(v)* reduction. The irreversible reduction of Np(v)* proceeds with small overpotential at the column electrode with the GC fiber working electrode at which the electron transfer is relatively fast (GC fiber used to record curves in Fig. 6) and, hence, it merges into the reduction of NpO_2^+ to Np(IV), which explains why the reduction of NpO_2^+ was observed as one wave corresponding to $n = 2$ [cf. curve 1(Np) in Fig. 6].

Though two-step reduction of PuO_2^+ has not been observed in nitric, perchloric and sulphuric acids, such species as PuO^{2+} and Pu(v)*, similar to NpO^{2+} and Np(v)*, are expected to participate in the reduction of PuO_2^+ to Pu^{3+}.

5 CONCLUSIONS

The E°s and mechanisms of the redox processes of the U, Np or Pu ions in acidic aqueous solutions were re-evaluated in the present paper, taking into account the results obtained by applying modern solution chemical theories and electrochemical techniques. It has been pointed out that E°s which had been widely accepted included considerable ambiguity arising mainly from the inaccurate activity corrections. The processes of irreversible reductions of MO_2^+ to M^{4+} or disproportionations of MO_2^+ have been estimated not to be simple, as believed previously, and new species have been proposed as the intermediates in these reactions.

It is hard to say that the redox behavior of the U, Np or Pu ions have been understood fully even in the most widely investigated solutions, i.e. acidic aqueous solutions, as described in this paper. The understanding of the behavior is still less in neutral or weakly basic solutions that might be very important in the field of the disposal of the nuclear waste in soil or sea. Therefore, the further extensive investigations leading to the more detail understanding of redox behaviors of actinide ions in not only acidic but also neutral or weakly basic aqueous solutions are required for the safety development of nuclear energy.

6 LIST OF SYMBOLS AND ABBREVIATIONS

a	activity
c	concentration
D	Debye–Hückel term
DME	dropping mercury electrode
E°	standard redox potential
$E^{\circ\prime}$	formal potential
$E_{1/2}$	half-wave potential in polarogram
$E_{\tau/4}$	quarter-wave potential in chronopotentiogram
F	Faraday constant
f	flow rate of sample solution in flow coulometry
GC	glassy carbon
i	objective ion
I	instantaneous current in coulopotentiogram
i_l	limiting current in polarogram or voltammogram
I_{la}	anodic limiting current in coulopotentiogram
I_{lc}	cathodic limiting current in coulopotentiogram
j	ion of which charge is opposite to that of i
k_s	standard rate constant
L	length of a column electrode

M	U, Np, Pu or Am
m_j	molality of j
MSE	mercuric sulphate electrode
n	number of electrons involved in a redox reaction
NHE	normal hydrogen electrode
O	oxidant
R	reductant
R	gas constant
r.p.m.	revolutions per minute
SCE	saturated calomel electrode
SIT	specific ionic interaction theory
SSE	silver/silver chloride electrode
z	charge of an ion
α	transfer coefficient
γ	activity coefficient
ΔG°	standard Gibbs free energy
ϵ(i,j)	specific interaction coefficients between i and all of j
κ	cell constant of a column electrode
μ	ionic strength
ν	scan rate of potential
ω	rotation rate of a electrode

REFERENCES

1 Ch. Riglet, P. Vitorge, I. Grenthe. *Inorg. Chim. Acta* **133**, 323–329 (1987).

2 Ch. Riglet, P. Robouch, P. Vitorge. *Radiochim. Acta* **46**, 85–94 (1989).

3 W. M. Latimer. *Oxidation Potentials*, 2nd edn. Prentice Hall. Englewood Cliffs, NJ (1952).

4 L. J. Nugent, R. D. Baybarz, J. L. Burnett, J. L. Ryan. *J. Phys. Chem.* **77**, 1528–1539 (1973).

5 L. J. Nugent. *J. Inorg. Nucl. Chem.* **37**, 1767–1770 (1975).

6 S. G. Bratsch, J. J. Lagowski. *J. Phys. Chem.* **89**, 3310–3316 (1985).

7 S. G. Bratsch, J. J. Lagowski. *J. Phys. Chem.* **89**, 3317–3319 (1985).

8 S. G. Bratsch, J. J. Lagowski. *J. Phys. Chem.* **90**, 307–312 (1986).

9 L. Martinot, J. Fuger. In *Standard Potentials in Aqueous Solution* (A. J. Bard, R. Parsons, J. Jordan, eds), p. 631. Marcel Dekker, New York (1985).

10 L. R. Morss. In *The Chemistry of the Actinide Elements* (J. J. Katz, G. T. Seaborg, L. R. Morss, eds), Vol. 2, p. 1278. Chapman & Hall, London (1986).

11 K. S. Pitzer. In *Activity Coefficients in Electrolyte Solutions* (R. M. Pytkowicz, ed.), Vol. 1, p. 157. CRC, Boca Raton (1979).

12 R. E. Connick, W. H. Mcvey. *J. Am. Chem. Soc.* **73**, 1798–1804 (1951).

13 D. Cohen, J. C. Hindman. *J. Am. Chem. Soc.* **74**, 4679–4682 (1952).

14 D. Cohen, J. C. Hindman. *J. Am. Chem. Soc.* **74**, 4682–4685 (1952).

15 S. W. Rabideau. *J. Am. Chem. Soc.* **78**, 2705–2507 (1956).

16 J. Fuger, F. L. Oetting. In *The Chemical Thermodynamics of Actinide Elements and Compounds*. Part 2. *The Actinide Aqueous Ions*. IAEA, Vienna (1976).

17 J. R. Brand, J. W. Cobble. *Inorg. Chem.* **9**, 912–917 (1970).

18 J. C. Sullivan, J. C. Hindman, A. J. Zielen. *J. Am. Chem. Soc.* **83**, 3373–3378 (1961).

19 L. Ciavatta. *Ann. Chim (Rome)* **70**, 551–567 (1980).

20 I. Grenthe, D. Ferri, F. Salvatore, G. Riccio. *J. Chem. Soc., Dalton Trans.* 2439–2443 (1984).

21 S. Ahrland, J. O. Liljenzin, J. Rydberg. In *Comprehensive Inorganic Chemistry* (J. C. Bailar, H. J. Emeleus, R. Nyholm, A. F. Trotman-Dickenson, eds), p. 465. Pergamon Press, Oxford (1973).

22 K. A. Kraus, F. Nelson, G. L. Johnson. *J. Am. Chem. Soc.* **71**, 2510–2517 (1949).

23 K. A. Kraus, F. Nelson. *J. Am. Chem. Soc.* **71**, 2517–2522 (1949).

24 K. Spahiu. *Acta Chem. Scand.* **A39**, 33–45 (1985).

25 K. Schwabe, D. Nebel. *Z. Phys. Chem.* **220**, 339–354 (1962).

26 S. W. Rabideau, J. F. Lemons. *J. Am. Chem. Soc.* **73**, 2895–2899 (1951).

27 E. S. Kritchevsky, J. C. Hindman. *J. Am. Chem. Soc.* **71**, 2096–2103 (1949).

28 S. G. Bratsch. *J. Phys. Chem. Ref. Data* **18**, 1–21 (1989).

29 D. J. McEwen, T. de Vries. *Anal. Chem.* **31**, 1347–1351 (1959).

30 R. C. Propst. *Anal. Chem.* **43**, 994–999 (1971).

31 D. Cohen. *J. Inorg. Nucl. Chem.* **18**, 207–210 (1961).

32 S. Kihara. *J. Electroanal. Chem.* **45**, 45–58 (1973).

33 H. Aoyagi, Z. Yoshida, S. Kihara. *Anal. Chem.* **59**, 400–405 (1987).

34 Z. Yoshida, H. Aoyagi, S. Kihara. *Fresenius J. Anal. Chem.* **340**, 403–409 (1991).

35 S. Kihara, Z. Yoshida, H. Aoyagi. *Bunseki Kagaku* **40**, 309–323 (1991).

36 P. Herasymenko. *Chem. Listy* **19**, 272–279 (1925).

37 G. Booman, J. E. Rein, C. F. Metz, G. R. Waterbury. In *Treatise on Analytical Chemistry*, Part 2. *Analytical Chemistry of the Elements* (I. M. Kolthoff, P. J. Elving, eds), Vol. 9, p. 1. John Wiley and Sons, New York (1962).

38 W. E. Harris, I. M. Kolthoff. *J. Am. Chem. Soc.* **67**, 1484–1491 (1945).

39 H. G. Heal. *Nature* **157**, 225 (1946).

40 I. M. Kolthoff, W. E. Harris. *J. Am. Chem. Soc.* **68**, 1175–1179 (1946).

41 D. M. H. Kern, E. F. Orlemann. *J. Am. Chem. Soc.* **71**, 2102–2106 (1949).

42 E. F. Orlemann, D. M. H. Kern. *J. Am. Chem. Soc.* **15**, 3058–3063 (1953).

43 S. Casadio, L. Lorenzini. *Anal. Lett.* **6**, 809–820 (1973).

44 K. A. Kraus, H. Nelson. *J. Am. Chem. Soc.* **72**, 3901–3906 (1950).

45 H. Imai. *Bull. Chem. Soc. Jpn.* **30**, 873–881 (1957).

46 M. A. Ghandour, R. A. Abo-Doma, E. A. Gomaa. *Electrochim. Acta* **27**, 159–163 (1982).

47 I. M. Kolthoff, W. E. Harris, G. Matsuyama. *J. Am. Chem. Soc.* **66**, 1782–1786 (1944).

48 H. G. Heal. *Trans. Faraday Soc.* **45**, 1–11 (1949).

49 G. A. Inamdar, R. G. Dhaneshwer. *Proc. The International Symposium on Uranium Technology*, p. 389, Bahbha Atomic Research Center, Bombay, India (1989).

50 S. P. Best, J. H. Clark, R. P. Cooney. *Inorg. Chim. Acta* **145**, 141–147 (1988).

51 R. E. Dueber, A. M. Bond, P. G. Dickens. *J. Electrochem. Soc.* **141**, 311–316 (1994).

52 K. E. Kacemi, B. Tyburce, S. Belcadi. *Electrochim. Acta* **27**, 729–733 (1982).

53 J. C. Hindman, E. S. Kritchevsky. *J. Am. Chem. Soc.* **72**, 953–956 (1950).

54 J. C. Hindman, L. B. Magnusson, T. J. La Chapelle. *J. Am. Chem. Soc.* **71**, 687–693 (1949).

55 M. Cl. Musikas. *Radiochim. Acta* **1**, 92–98 (1963).

56 C. Degueldre. Thesis, University of Liege (1972), cited in [57].

57 L. Martinot. In *Encyclopedia of Electrochemistry of the Elements* (A. J. Bard, ed.), p. 149. Marcel Dekker, New York (1978).

58 C. E. Plock. *J. Electroanal. Chem.* **18**, 289–293 (1968).

59 S. Casadio, F. Orlandini. *J. Electroanal. Chem.* **33**, 212–215 (1971).

60 U. Niese, J. Vecernik. *Isotopenpraxis* **18**, 191–192 (1981).

61 J. C. Hindman. US Report CN-2289, November 1, 1 (1944).

62 B. G. Harvey, H. G. Heal, A. G. Maddock, E. L. Rowley. *J. Am. Chem. Soc.* **69**, 1010–1021 (1947).

63 K. Koyama. *Anal. Chem.* **32**, 523–524 (1960).

64 D. G. Peters, W. D. Shults. *J. Electroanal. Chem.* **8**, 200–229 (1964).

65 I. V. Moiseev, A. Ya. Kuperman, N. N. Borodina. *Radiokhimiya* **17**, 410–415 (1975).

66 S. Kihara. *J. Electroanal. Chem.* **45**, 31–44 (1973).

67 T. Fujinaga, S. Kihara. *CRC Crit. Rev. Anal. Chem.* **6**, 223–254 (1977).

68 S. Kihara, Z. Yoshida, H. Muto, H. Aoyagi, Y. Baba, H. Hashitani. *Anal. Chem.* **52**, 1601–1606 (1980).

69 N. I. Udal'tsova. In *Analytical Chemistry of Uranium* (D. I. Ryabchikov, M. M. Senyavin, eds), Series *Analytical Chemistry of Elements* (A. P. Vinogradov, Chief ed.), Chap. II, p. 8. Academy of Sciences of the USSR, Translated by Israel Program for Scientific Translations, Jerusalem, (1963).

70 V. A. Mikhailov. In *Analytical Chemistry of Neptunium* (P. N. Palei, ed.), Series *Analytical Chemistry of Elements* (A. P. Vinogradov, Chief ed.), Chap. II, p. 10. Academy of Sciences of the USSR, Translated by Israel Program for Scientific Translations, Jerusalem (1973).

71 Z. Yoshida, H. Aoyagi, Y. Kato, Y. Li, S. Kihara. *Proc. The Third International Symposium on Advanced Nuclear Energy Research—Global Environment and Nuclear Energy*, pp. 268–272. Japan Atomic Energy Research Institute, Ibaraki, Japan (1991).

72 J. A. Fahey. In *The Chemistry of the Actinide Elements* (J. J. Katz, G. T. Seaborg, L. R. Morss, eds), 2nd edn. Vol. 1, Chap. 6, p. 471. Chapman & Hall (1986).

73 K. A. Kraus, G. E. Moore. In *The Transuranium Elements* (G. T. Seaborg, J. J. Katz, W. M. Manning, eds), *Natl. Nucl. Energy Ser. IV*, Vol. 14B, p. 550, McGraw-Hill, New York (1949).

74 R. Kraus. In *The Transuranium Elements* (G. T. Seaborg, J. J. Katz, W. M. Manning, eds), *Natl. Nucl. Energy Ser. IV*, Vol. 14B, p. 241. McGraw-Hill, New York (1949).

75 F. David. *J. Less-Common Met.* **121**, 27–42 (1986).

76 R. E. Connick. In *The Actinide Elements* (G. T. Seaborg, J. J. Katz, eds), *Natl. Nucl. Energy Ser. IV*, Vol. 14A, p. 234. McGraw-Hill, New York (1954).

77 J. B. Sobkowski, S. Minc. *J. Inorg. Nucl. Chem.* **19**, 101–106 (1961).

78 J. B. Sobkowski. *J. Inorg. Nucl. Chem.* **23**, 81–90 (1961).

79 M. Cl. Musikas, F. Couffin, M. Marteau. *J. Chim. Phys.* **71**, 641–648 (1974).

80 W. E. Harris. Thesis, University of Minnesota (1945), cited in Ref. [37].

81 S. W. Sheel. US Report CC-2771 (1945).

82 Y. V. Morachevskii, A. A. Sakharov. *Z. Anal. Khim.* **13**, 83–87 (1958).

83 N. B. Mikheev. *Radiochim. Acta* **32**, 69–80 (1983).

7 APPENDIX

Flow coulometry at the column electrode

The electrolysis with the column electrode in a flow system is called flow coulometry. The cell configuration for flow coulometry is illustrated in Fig. 4 [33,67,68]. The working electrode of the column electrode is composed of a bundle of fine glassy carbon fibers ($\approx 10\,\mu$m in diameter) packed in a porous Vycor® glass cylinder (e.g. 8 mm i.d., 10 mm o.d. and 50 mm long) which works as an electrolytic diaphragm. The electrolysis is performed by forcing the sample solution to flow through the column electrode and by applying the electrode potential with the aid of a platinum counter electrode and a saturated KCl Ag/AgCl or 1 M LiCl Ag/AgCl (SSE) reference electrode set outside of the diaphragm cylinder.

For multistep flow coulometry, an appropriate number of column electrodes are connected in series closely. The time required to transfer the solution from one column to the succeeding column is at the least 0.01 s though it depends on the flow rate of the solution and the distance between two column electrodes.

The limiting current (ampere), I_l, which is measured when the electrolysis is attained quantitatively, is given by

$$I_l = n\,F\,f\,c \tag{A1}$$

where, n, F, f and c are the number of electrons involved in the reaction, the Faraday constant, the flow rate of the solution (dm^3/s) and the concentration of the substance studied (mol/dm^3), respectively. Equation A1 indicates that the concentration of the objective species can be determined directly from I_l when f is controlled at constant.

The current-potential curve at the column electrode [67,68], which is called as the coulopotentiogram, is given by Eqn A3 when the electrode reaction Eqn A2 is reversible and both oxidant, O, and reductant, R, are soluble in solution.

$$O + ne \rightleftharpoons R \tag{A2}$$

$$E = E^\circ - (RT/nF)\ \ln\ (D_O/D_R)^{2/3} + (RT/nF)\ln[(I_{lc} - I)/(I - I_{la})] \tag{A3}$$

where E, E°, R and T are the electrode potential, the standard redox potential, the gas constant and temperature, respectively. D_O and D_R are diffusion constants of O and R. I, I_{lc} and I_{la} are the instantaneous current, the cathodic limiting current and the anodic limiting current, respectively.

The half-wave potential, $E_{1/2}$, is expressed as

$$E_{1/2} = E^\circ - (RT/nF)\ln(D_O/D_R)^{2/3} \tag{A4}$$

When the electrode reaction Eqn A2 is totally irreversible, the coulopotentiogram for the cathodic process is represented by

$$E = E^\circ - (RT/\alpha nF)\left\{\ln(\kappa f/k_s L) + \ln[\ln[I_{lc}/(I_{lc} - I)]]\right\} \tag{A5}$$

where α, κ, k_s and L are the transfer coefficient, the cell constant, the standard rate constant and the column length, respectively.

The half-wave potential, $E_{1/2}$, is expressed as

$$E_{1/2} = E^\circ - (RT/\alpha nF)\left\{\ln(\kappa f/k_s L) + \text{constant}\right\} \tag{A6}$$

Equations A4 and A6 indicate that $E_{1/2}$ is independent of f and L when the electrode reaction is reversible, while $E_{1/2}$ depends on f and L when the electrode reaction is irreversible.